Uranium in groundwater and its potential as a natural contaminant in the Cherokee Basin, southeastern Kansas.

by

Fidelis Chinaemelum Onwuagba

B.S., Nnamdi Azikiwe University, 2021

A THESIS

submitted in partial fulfillment of the requirements for the degree

MASTER OF SCIENCE

Department of Geology
College of Arts and Science

KANSAS STATE UNIVERSITY
Manhattan, Kansas

2024

Approved by:

Dr. Karin Goldberg
Major professor

Copyright

Abstract

Safe, easily accessible, clean, and potable water is critical for public health. The ingestion of radioactive nuclides such as uranium has been associated with renal and cancer-related issues in humans. Many previous studies have focused on anthropogenic uranium contamination. Here, we examined the potential for natural uranium contamination from water-rock interaction in black shales. After uranium ores, black shales are the second most important uranium source. Immobile uranium can be mobilized and absorbed into groundwater under ideal geochemical circumstances depending on redox status, carbonate speciation, and alkalinity. The sedimentary succession in the Cherokee Basin in southeastern Kansas includes several black shales interbedded with limestones. Gamma-ray logs from oil and gas wells revealed a very high level of radioactivity in the black shales, reaching 740 API (units of gamma-ray radiation) in some areas, suggesting the presence of radioactive uranium in these rocks. We collected and chemically analyzed groundwater samples from domestic wells screened in the Ozark carbonate aquifer to examine whether these units are sources of groundwater uranium contamination. The samples had a pH of 6.27 to 7.96 and alkalinity ranging from 0.6 to 18 mM. Some samples had high sulfate and nitrate (as N) concentrations, up to 373 mg/L and 22 mg/L, respectively. This study also investigated the connection between black shales and uranium concentrations in groundwater and a possible link to cancer incidence in the study area. Uranium levels were generally low; however, we found numerous other redox-sensitive solutes, specifically mercury, manganese, and iron, in concentrations of 0.02 mg/L, 3.3 mg/L, and 11 mg/L, respectively. These are well above the primary or secondary U.S. EPA and WHO standards for drinking water and are known to be directly or indirectly linked to certain types of cancer in humans, including bladder, brain and nervous system, kidney, blood, lung and bronchus, liver, and pancreas cancer. These results have

implications for the best practices for household water well owners and target depths for potential water well owners to ensure drinking water quality, consequently reducing the prevalence of cancer associated with the consumption of contaminated groundwater.

Table of Contents

List of Figures

List of Tables

Acknowledgments

I would like to give thanks to God almighty for guiding me through this journey and granting me the strength, wisdom, and perseverance needed to complete this thesis.

I extend my sincere gratitude to the Department of Geology at Kansas State University, especially the Department Head, Dr. Pamela Kempton, for their unwavering support and resources throughout my academic journey at K-State.

I am deeply indebted to my academic advisor, Dr. Karin Goldberg, whose guidance, mentorship, and unending support have been instrumental in shaping this research. Dr. Goldberg's dedication and wisdom have been invaluable to me, and her role in this journey cannot be overstated.

I also extend my heartfelt gratitude to my advisory committee members, Dr. Matthew Kirk, Dr. Behzad Ghanbarian, and Dr. Walter Dodds, for their invaluable guidance, encouragement, and scholarly insights that have enriched this research.

Special thanks to Sam Galliardt for her assistance throughout this research, from the preliminary studies to the fieldwork and the laboratory analysis; you were fantastic! Also, I thank my friends and colleagues who have offered various forms of assistance, encouragement, and camaraderie throughout this endeavor. Your support has been invaluable.

I want to express my appreciation to the funding sources that made this research possible, including the American Chemical Society, the Johnson Cancer Research Center, the American Association of Petroleum Geologists, The Geological Society of America, the Society of Exploration Geophysicists, the Kansas Geologic Foundation, the Association of Earth Science Club of Greater Kansas City Inc., and the K-State Graduate School for their financial support and belief in the importance of scientific inquiry.

Lastly, I am grateful to Kansas State University for providing an enriching academic environment for my scholarly and research pursuits.

Dedication

I dedicate this thesis to my beloved family for their unwavering love, encouragement, and sacrifices. Their steadfast support has been the guiding light to my academic journey. This accomplishment is as much theirs as it is mine.

To all victims and survivors of cancer, your strength, resilience, and hope inspire me every day. I hope this research contributes to a future free from Cancer…Cheers to a cancer-free future!!!

Chapter 1 - Introduction

Uranium is a naturally occurring radionuclide usually found in organic carbon-rich regions due to the weathering of igneous rock materials (Adler, 1974; Nolan & Weber, 2015). Fly ash from uranium-bearing coal is particularly rich in uranium, and several proposals have been made to "mine" this waste product for its uranium content (Maslov *et al*., 2010). Most of the uranium exists in soils and sediments as insoluble, reduced U^{+4} minerals, e.g., uraninite and coffinite (Duff *et al*., 1999; Alam, 2014; Nolan & Weber, 2015), which are likely to be associated with volcanic rocks or organic-rich rocks, and as such are generally immobile or insoluble in suboxic groundwater. It has been recognized that exposing reduced U^{+4} minerals to oxidizing groundwater leads to oxidative dissolution, producing aqueous or dissolved U^{+6} species and rendering uranium mobile (Cumberland *et al*., 2016). The primary determinants of uranium behavior in ore systems are pH, Eh, its oxidation state (U^{+4}, U^{+6}), and the abundance of CO_3^{2-} ions (Cumberland *et al.*, 2016). In its +4-oxidation state (U^{+4}), uranium is less soluble and forms more stable compounds than in its +6-oxidation state (U^{+6}), which is more readily mobilized (Nolan & Weber, 2015). According to Nolan and Webber (2015), U^{+6} strongly adsorbs into sedimentary matrices at a pH of about 6 – 10; however, mineral dissolution reactions will increase dissolved carbonate concentrations, favoring the formation of soluble U^{+6} carbonate species, including U^{+6} $CaCO_3$ species, and adsorption becomes insignificant (Stewart, 2010). Thus, redox chemistry (oxidation state) and carbonate alkalinity are recognized as primary factors controlling uranium mobility. Studies have shown that uranium inclusion in groundwater is primarily attributed to anthropogenic activities such as mining, nuclear testing, milling, disposal of radioactive nuclear wastes, and hydraulic fracturing (Nolan & Weber, 2015). These activities adversely affect the environment, particularly

groundwater, but in addition to these, chemical elements and compounds derived from geological materials and processes also influence water quality (Hasan, 2021).

1.1 Statement of Problem

Uranium has been identified as a nephrotoxic metal (kidney toxicant), exerting toxic effects by chemical action, mainly in the proximal tubules in humans and animals (Keith *et al.,* 2013; Nolan *et al.,* 2021). Besides being toxic to the kidneys, chronic exposure to uranium is also associated with several adverse health outcomes, including liver damage, cardiovascular diseases (Ravelli *et al*., 2022), and cancer (Tirmarche, 2004) (Fig. 1.1). According to the United States Environmental Protection Agency, it is estimated that about 4% of private groundwater wells in the United States have uranium concentrations exceeding the EPA acceptable Maximum Contamination Level for drinking water (0.03 mg/L) (DeSimone *et al*., 2014). Most US residents rely on public drinking water systems, with most residents (approximately 90%) relying specifically on community water systems (CWSs) that serve the same population year-round (Ravelli *et al*., 2022). However, the rural community often consumes water from domestic wells, largely unregulated and untested.

Uranium contamination of ground and surface water has been detected at numerous sites worldwide, including agricultural evaporation ponds (Bradford *et al*., 1990), nuclear weapons manufacturing areas, and mine tailing sites (Riley *et al*., 1992). In 1950, the US Public Health Service began a comprehensive study of uranium miners, leading to the first publication of a statistical correlation between cancer and uranium mining, released in 1962 (Dawson, 2007). According to Ravalli *et al.* (2022), drinking water access and quality disparities are related to structural inequalities in the built environment, land use, and differences in the geological environment.

1.2 Study Area

The study area includes Bourbon, Crawford, and Cherokee Counties, located in the Southeastern corner of Kansas (Fig. 1.2), where abundant organic-rich shales and carbonate rocks are found. The dominant land use in the area is agriculture. Agricultural practices are more intense in Bourbon County, the most rural county among the studied counties. The groundwater source in the area is the Ozark aquifer, consisting of a thick sequence of horizontal to southward-dipping limestones and dolomites, containing some sandstones, shales, and chert (Ranken, 1998), with rock units ranging from Cambrian to Mississippian. This confined aquifer is the primary portable water source in southeastern Kansas (Fig. 1.2).

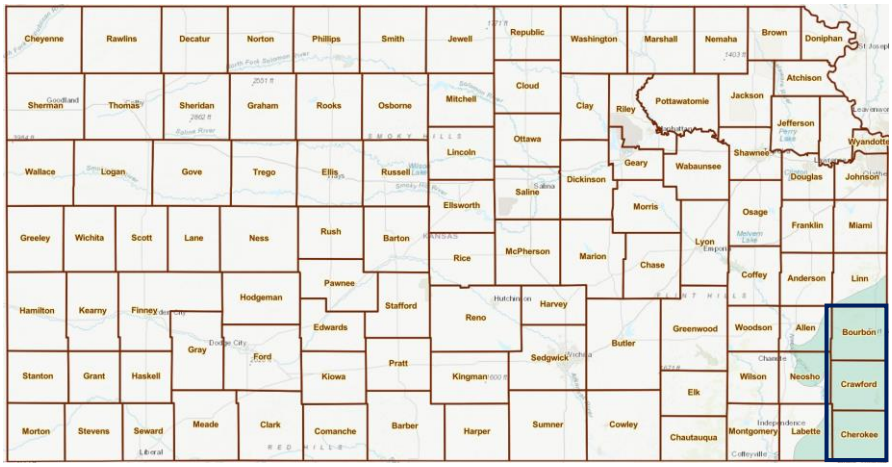

Figure 1.1: Location of the study area (highlighted in blue) in southeast Kansas (Kansas Geological Survey).

Geologically, the Ozark aquifer is in close contact with several black shales and bituminous coal deposits, acting as confining units (Fig. 1.3). The common interbedding between limestones and black shales can be observed in outcrops along some of the roads in the area (Fig. 1.4).

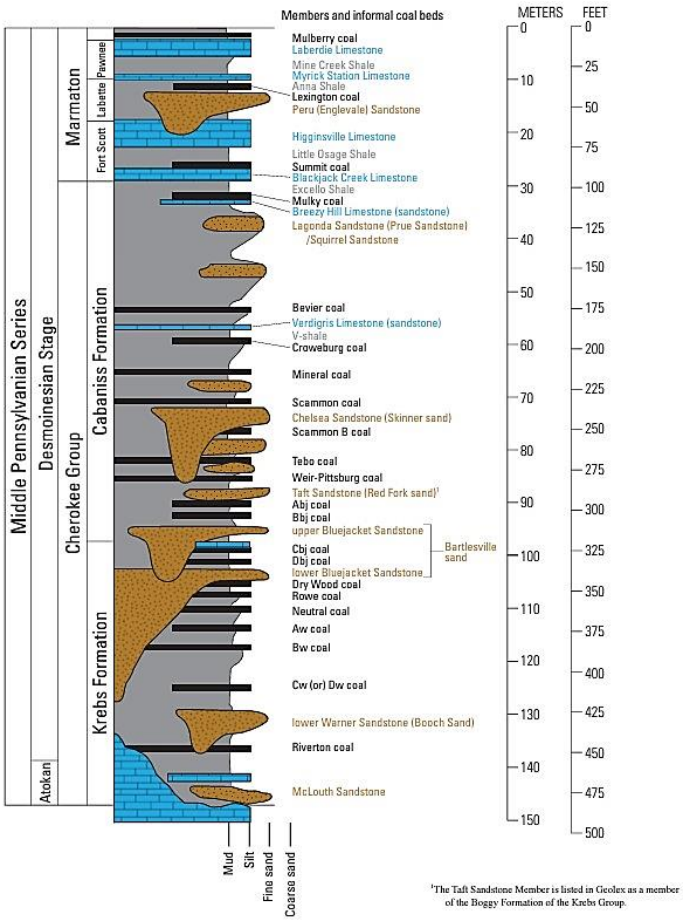

Figure 1.2: Desmoinesian Cherokee and Marmaton Groups in the Cherokee Platform area of southeastern Kansas and northeastern Oklahoma (Drake & Hatch, 2021), showing the interbedding between organic-rich rocks and carbonate rocks of the Ozark Aquifers.

Figure 1.3: Outcrop on a roadcut along interstate 69, showing sharp contact between a limestone layer (above) and black shales (below) in Fort Scott, Bourbon County.

Organic-rich rocks such as black shales and coals have uranium concentrations up to hundreds of parts per million (Cumberland *et al.*, 2016) (Table 1.1). Depending on the chemical composition of the aquifer and the level of alkalinity, the interaction between groundwater and these rocks could mobilize uranium species into the groundwater.

Table 1.1: Average uranium concentration in ores, rocks, and waters (reproduced from Belaram et al., 2022).

Materials	Concentrations (µg/g)
High-grade orebody (>2%U)	>20,000
Low-grade orebody (~0.1%U)	1000
Average granite	4
Average volcanic rock	20-200
Average sedimentary rock	2
Average black shale	50-250
Average Earth's crust	2.8
Sea water	0.003
Groundwater	>0.001-0.008

This research hypothesized that the groundwater system in the Cherokee Basin of southeast Kansas had a high concentration of uranium due to the interaction between groundwater in the Ozark aquifers and organic-rich rocks in the area, leading to natural contamination of the water resources. The impermeable nature of black shales restricts groundwater interaction to interface along limestone-shale contacts. Over time, uranium may gradually dissolve into groundwater through diffusion and advection, provided the geochemical conditions are favorable. The potential uranium contamination would have profound health implications for the human population supplied by domestic wells in the study area.

Hence, the goal of this study was to investigate a potential correlation between the geology of the area (specifically the occurrence of black shales) and the uranium concentration in groundwater collected from domestic wells. Because of the radioactive properties of uranium, the

secondary goal was to investigate whether the uranium concentration in groundwater is related to the incidence of cancer.

1.3 Significance of Research

Research has been carried out to understand uranium's origin, geochemistry, and mobility in groundwater (Duff *et al*., 1999; Alam, 2014; Nolan & Weber, 2015; Cumberland *et al.*, 2016; Bonotto *et al.*, 2019; Ravelli *et al.*, 2022;). Previous studies have also shown that high concentrations of uranium in drinking water are associated with severe health complications (Tirmarche, 2004; Keith *et al.*, 2013; Nolan *et al.*, 2021; Ravelli *et al*., 2022). However, studies that investigate the link between geology and the presence, concentration, and distribution of this toxic radionuclide in groundwater are limited, focusing primarily on granitic terrains (Brindha, 2013; Lapworth *et al*., 2021; Baják *et al.*, 2022).

This research aimed to contribute to the field of Medical Geology, which focuses on studying how geologic materials and environmental processes affect human health. Specifically, it investigated the potential risk that organic-rich rocks may pose to groundwater, resulting in high cancer incidence in the population consuming this water. This project has a national relevance, given the broad area of the United States covered by these rocks (Fig 1.5), and the coincidence between high cancer incidence and the occurrence of black shales (Fig. 1.6).

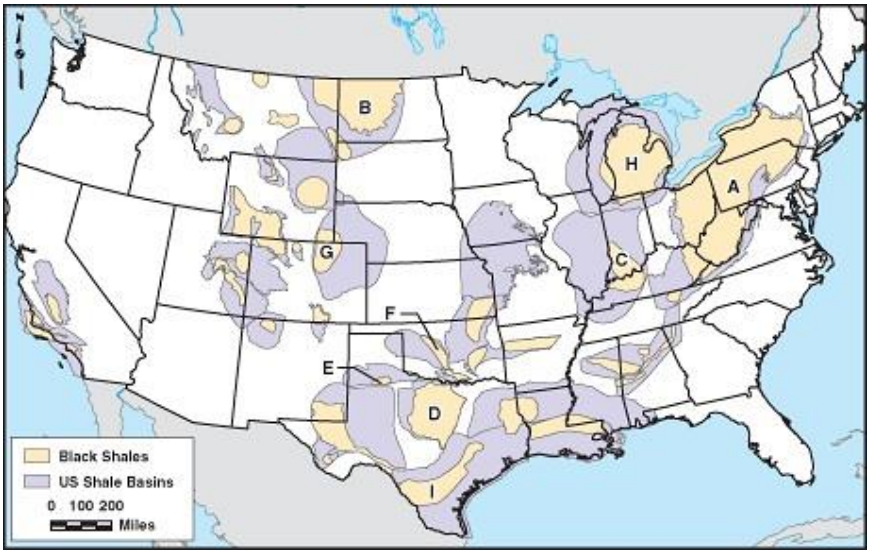

Figure 1.4: Distribution of black shales across the United States (Flewelling & Sharma, 2013).

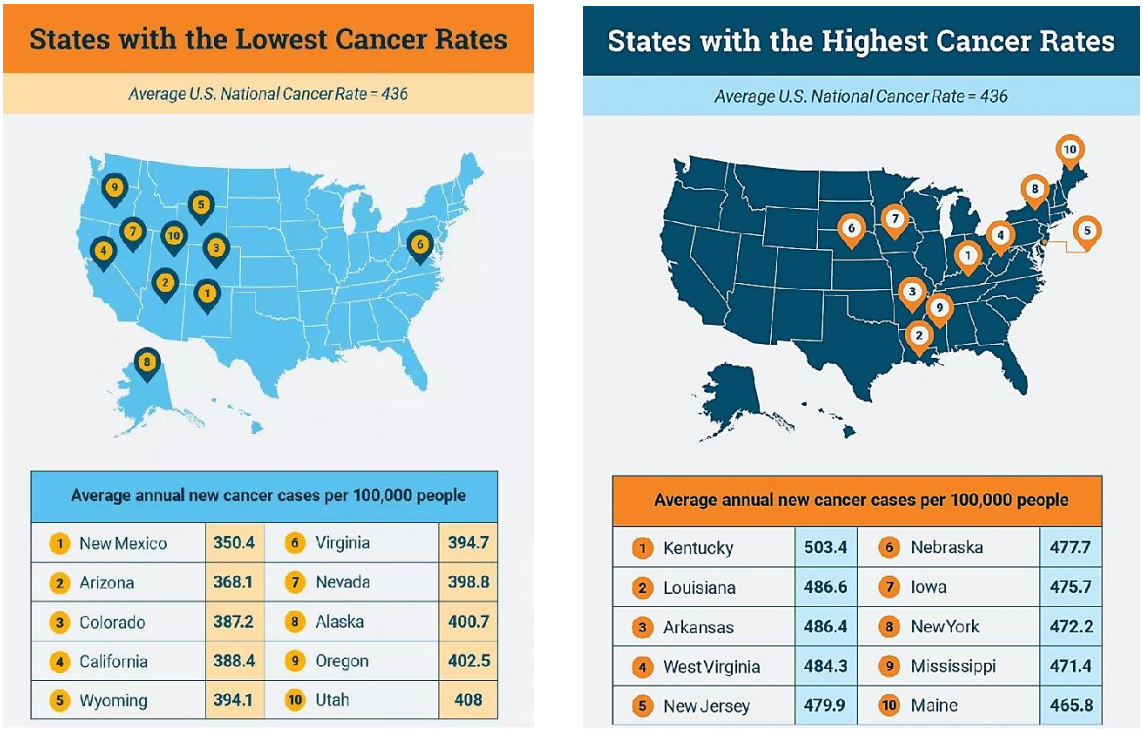

Figure 1.5: Cancer incidence across the U.S. (National Cancer Database). The states with the lowest cancer rates (left) (in the west) are not abundant in black shales, whereas those with the highest cancer rates (right) (in the east) have abundant black shales.

Although the evidence is anecdotal, it underscored the importance of obtaining data on uranium concentrations in groundwater. This information is crucial to water-well owners and public water treatment facilities to ensure the quality of domestic drinking water, reducing the amount of uranium-related health issues in any given area.

1.3 Geologic Setting

Kansas has been a part of a stable craton since at least the beginning of the Paleozoic, some 550 m.y. ago (Newell, 2013). Significant uplift and subsidence occurred episodically throughout the Phanerozoic, separated by periods of gradual deformation (Newell, 2013). These periods of active tectonic movement were usually times of low sea level and subsequent erosion (Newell, 2013). The record of sedimentation in Kansas is thus episodic, interrupted by significant unconformities. Most of these major basins, arches, and lesser structures are a consequence of the major deformation that occurred during the Early Pennsylvanian (pre-Desmoinesian). Earlier uplifts and basins which significantly affected the distribution of lower Paleozoic strata lie buried in the subsurface. For example, the Salina and Forest City Basins were originally part of a much more extensive basin (the North Kansas Basin) during the Ordovician through Late Mississippian, when sedimentary rocks from the Simpson, Viola, Maquoketa, and Hunton Formations thickened northward toward a depocenter in Nebraska and Iowa. The basin was bordered on the south by the broad Chautauqua Arch, now the site of the Cherokee Basin, and to the west by the ancestral Central Kansas Uplift (Newell, 2013; Merriam, 1963).

Cherokee Basin

The Cherokee Basin is an intracratonic depression that is part of the Pennsylvanian-age Western Interior Basin (Tedesco, 2014) and covers about 8,400 square miles in southeastern Kansas and northeastern Oklahoma (Kansas Geologic Survey, 2006). Mississippian rocks, the

oldest exposed in Kansas, crop out in Cherokee County, in the extreme southeastern corner of the state, while Pennsylvanian and Permian rocks are exposed over the rest of the basin. These sediments undergo facies changes southward into Oklahoma, making correlation of individual beds difficult. The maximum sedimentary sequence is about 3,500 feet thick, and Lower Pennsylvanian beds overlie Cambrian-Ordovician and Ordovician rocks throughout most of the basin (Kansas Geological Survey, 2006).

Bourbon County

Bourbon County has a total area of 638 mi^2 (1,652 km^2) (West & Sawin, 2020; Bell & Fortner, 1981). The Kansas Geological Survey describes the local geology of Bourbon County as being mainly characterized by Pennsylvanian-age rocks and Holocene alluvium/stream terraces cropping out at the surface or directly underlying the soil and vegetation. The general orientation of these rocks is northeast-southwest, diagonally across the county, with the oldest (Cherokee Group) exposed in the southeastern corner and the eastern edge of the county, rocks of the Marmaton and Pleasanton Groups in the middle, and the youngest (Kansas City Group) rocks along the western edge (West & Sawin, 2020). These rocks include marine shales, sandstones, siltstones, fossiliferous limestones, and coal. The stratigraphic sequence in Bourbon County extends from below the Mineral coal bed in the Cabaniss Formation (Cherokee Group) to the lower part of the Cherryvale Shale (Kansas City Group) (Fig. 1.3).

Bourbon County is known for its coal-mining heritage. Coal has been mined from the upper Cherokee and Marmaton Groups, which occur near the surface in the eastern part of the county. Most of the mines were surface mines, although some underground mining operations were also conducted. Oil and gas are produced from about 30 active fields in Bourbon County (West & Sawin, 2020), almost exclusively from the Cherokee Group sandstones and coals. A few small

fields have produced some oil from the Mississippian carbonates. Limestone is quarried for aggregate from several Pennsylvanian formations throughout the county. The Bandera Sandstone Member of the Bandera Shale is quarried near Redfield for flagstone and building stone.

Crawford County

According to West & Sawin (2008), Crawford County has a total area of 595 mi^2 (1,541 km^2). Pennsylvanian sedimentary rocks (limestones, mudrocks, sandstones, and coals) crop out within the county and range in age from the lower Desmoneisian (Cherokee Group) to the lower Missourian (Kansas City Group) (Fig. 1.3). Similar to Bourbon County, the general orientation of these rocks is diagonally (NE-SW) across the county from the oldest (Cherokee Group), exposed in the southeastern corner of the county, to rocks of the Marmaton Pleasanton Groups across the middle, to the youngest (Kansas City Group) rocks in the northwestern corner. The rocks of the Cherokee Group are mostly siliciclastic (mudrocks and sandstones), with an occasional thin limestone layer. It is within this interval that most of the economically important coal beds occur. The lower Marmaton Group consists of siliciclastic and thick limestones; the upper Marmaton and Pleasanton Groups are mostly siliciclastic rocks with thin limestones; and the Kansas City Group consists of mudrocks and thick limestones. Crawford County is known for its coal-mining heritage. Other industries supported by mineral resources include bricks and tile plants and zinc smelters. Mudrocks provides the raw material for brick, tile, and other ceramic products. Coal for fuel attracted the zinc smelters, with the ore coming from Cherokee County and Missouri.

Cherokee County

According to Benninson (2002), Cherokee County is the informal stratotype for the Middle Pennsylvanian Cherokee Group. The group underlies much of the county, except for Mississippian

strata in the southeast corner and the Marmaton Group of the Upper Desmoinesian Series in its northwest corner.

Cherokee County is known for its rich mining heritage. According to a 2022 report by the Kansas Historical Society, coal mining in Kansas began in the 1650s. The coal deposits of southeast Kansas drew a large number of workers (including European miners) to the area in the 1880s and 1890s, who found jobs in the shallow shafts. After they learned that the red rusty coal near the surface could be striped mined and was good for cooking and blacksmithing, strip mining began in the 1870s and became the preferred method in the 1930s.

The black, oily coal buried under about 200 feet of sandstone was accessed through deep mining and was suited for fueling steam locomotives. Power shovels like Big Brutus were used to remove the layers of coal. However, the minerals had been depleted by the 1970s, and the mines closed in the 1980s due to high-sulfur coal being outlawed. During the history of mining in Kansas, more than 300 million tons of coal was processed. The available workforce helped the area become the industrial center of the state. In addition to coal, lead and zinc were mined economically and played a key role in supplying these minerals needed during World War I and World War II (Kansas Historical Society, 2018).

The recurrent interbedding of uranium-bearing black shales and coals with carbonate rocks (which supply CO_3^{-2} ions that may affect uranium behavior) in these counties makes this area the ideal location to investigate the potential connection between the geology and uranium remobilization to groundwater.

Chapter 2 - Methods

The project methodology included fieldwork and laboratory analyses. Fieldwork aimed at collecting water samples from water wells and measuring in-situ water properties across the study area. Water from the wells sampled wells serve various purposes, including domestic use, livestock feeding, irrigation, and public water supply. The depths of the sampled wells varied widely, ranging from 3.6 ft to 1150 ft, with water levels ranging from 2.1 ft to 365 m below the surface.

Laboratory analyses aimed at characterizing the chemical properties and trace element concentrations in water samples, as well as compiling geological and cancer data. A detailed description of the methods is found below.

2.1 Fieldwork

During two field campaigns carried out in the Spring and Summer of 2023, a total of 43 water samples were collected (41 from domestic wells and two from public water supplies), with 16 samples in Bourbon County, 7 in Crawford County (including the public water supply in the cities of Fort Scott and Frontenac) and 20 in Cherokee County. The uneven distribution of water samples was due to either the unavailability of operational wells or the unwillingness of well owners to grant access and authorization for sampling.

For each well sampled, its coordinates (longitude and latitude) and elevation were recorded using the GPS Waypoints application. The depth-to-water was measured using a Solinst® water level electronic meter. To access the water for sampling, we used either an electronic pump (Geo Control Pro electric air pump), yard hydrants, or a spigot outside the resident's home. The well was purged by allowing the water to run for about eight to ten minutes before sampling. In a few

wells, the use of an electric pump was not possible (due to its location, configuration, and accessibility), in which case the water samples were collected using a bailer. Depending on the diameter of the well, purging these wells was done with the bail, discarding the water between twenty to thirty times before collecting samples. Purging is done to eliminate stagnant water in the well, which is not representative of the water in the aquifer.

Once the well was properly purged, water samples were collected by allowing the water to flow through a 1000 ml graduated measuring cylinder, where water properties were measured in situ with the pre-calibrated field instruments. The flowing water ran past the measuring instruments inserted in the measuring cylinder; the devices took readings, ensuring minimal interaction of the water with the atmosphere. Through this procedure, temperature, pH, and electrical conductivity were measured in the field using an Oakton® portable water quality meter kit. A YSI Pro 2030 dissolved oxygen meter was also used to measure dissolved oxygen, percentage oxygen saturation, conductivity, specific conductance, and temperature again. Field instruments were carefully calibrated daily before sample collection (Fig. 2.1). The water quality meter was calibrated using an Oakton® pH buffer 4.01, 7.0, and 10.01 standard solution for the pH electrodes, and an ICCA potassium chloride conductivity, 1413 µs/cm at 25 °C standard solutions. The dissolved oxygen meter was calibrated using the same standard solution.

Figure 2.1: Calibration of field instruments prior to water sampling.

The instruments were allowed to take measurements of the water until a steady value for the respective parameters was reached before recording the readings. Once the physical-chemical parameters were measured and recorded, we proceeded with the collection of water samples. Three samples were collected at every location to test for trace elements, cations, and anions.

Prior to fieldwork, the new sample bottles were first prepared by immersing them in an acid bath (2% HCl solution) for twenty-four hours. The bottles were rinsed using 18 mΩ deionized water. Syringes and filters were also thoroughly rinsed using the 18 mΩ deionized water.

At each sample site, the 90 ml bottles were used to collect samples for anion and cation analysis, while the 30 ml bottle was used to collect samples for trace metal analysis. The bottles were filled using syringes and filters to ensure the collected samples did not contain particles that could affect the results of the analysis (Fig. 2.2). The collected samples from each site were tightly covered, labeled, and placed into a Ziploc bag and stored with ice in a cooler until the end of the day when they were transferred into a refrigerator back at the field base.

Figure 2.2: Sample collection in the field.

2.2 Geochemical Analyses

The samples collected were stored at the Geochemistry Lab in the Department of Geology, Kansas State University. Those collected for trace metal analysis were preserved by adding a drop of Fisher Chemical trace metal grade nitric acid. Samples for cation analysis were also acidified by adding two drops of the same acid to the samples. All the samples were stored in a refrigerator in the lab. Unacidified samples were subjected to alkalinity titrations, and samples for both cation and anion analyses were run through ion chromatography in the Geochemistry lab. Samples for trace metal analysis were shipped to the Redox Biology Center at the University of Nebraska-Lincoln for analysis. Trace-element concentrations were obtained through inductively coupled mass spectroscopy (ICP-MS).

The ion chromatography analysis was carried out using a Dionex ICS-11000 Ion Chromatograph device (Fig. 2.3), and the analysis results were processed using Chromeleon console software. We ran a dilute and undiluted version of all the samples during the analysis for precision. We carried out the alkalinity titration with a Thermoscientific OrionStar T910 automatic alkalinity titrator (Fig. 2.3) using a 0.02N sulfuric acid as the titrant. The titrator was first calibrated using the pH buffer solutions and diluted (1:4) $NaHCO_3$ solution.

Figure 2.3: Ion chromatographer (left) and alkalinity titrator (right).

2.3 Geochemical and Geospatial Modeling

Geochemical modeling was carried out to understand better the geochemistry of the groundwater in the study area. Field data (temperature, dissolved oxygen, pH, etc.), ion chromatography, and ICP-MS results served as the input for the simulations done with the Geochemist Workbench software.

Gamma-ray logs acquired from oil and gas wells drilled in the study area were extracted from the Kansas Geological Survey database (https://www.kgs.ku.edu/PRS/petroDB.html). The extracted gamma-ray logs were interpreted using the Petrel® 2018 software to calculate the

cumulative thickness of black shales within the depth of 0 ft - 300 ft across the study area using 150 API as a cut-off to discriminate between black shales and other lithologies. The data was used to plot an isopach map using Surfer® software.

To examine the spatial distribution of the potential contaminants in the study area, a two-dimensional model was created with the Surfer® software using the data from the ion chromatography and ICP-MS analysis.

Various plots were made using the Geochemists Workbench software and Python programming language.

2.4 Statistical Analysis

Statistical regression analysis was carried out using the SAS® software and Python programming language to investigate a potential correlation between thickness of black shales (extracted from the gamma-ray logs), groundwater geochemistry (results from ion chromatography and ICP-MS analyses) and cancer incidence. Cancer data were extracted from public databases such as the National Cancer Institute (https://gis.cancer.gov/canceratlas/), American Cancer Society (https://cancerstatisticscenter.cancer.org). Kansas Department of Health and Environment (https://maps.kdhe.state.ks.us) and Kansas Health Matters (https://www.kansashealthmatters.org). Data on different kinds of cancer were compiled to compare the three studied counties with the rest of the State of Kansas and the rest of the U.S. Cancer data spanned the interval of 2013-2017.

Chapter 3 - Results

3.1 Geophysical Analysis

The presence of highly radioactive lithologies (black shales) interbedded with less radioactive lithologies (carbonates and sands) was revealed by gamma ray log signatures. API values in the area ranged from 402.24 to 702.64 in some places (Fig. 3.1). Gamma ray data is provided in Appendix A.1.

The compilation of gamma ray log data from 88 wells in the study area allowed the construction of an isopach map of the cumulative thickness of black shales to the depth of 300 feet in the Bourbon and Crawford counties (Fig. 3.2). There was no data for the Cherokee County.

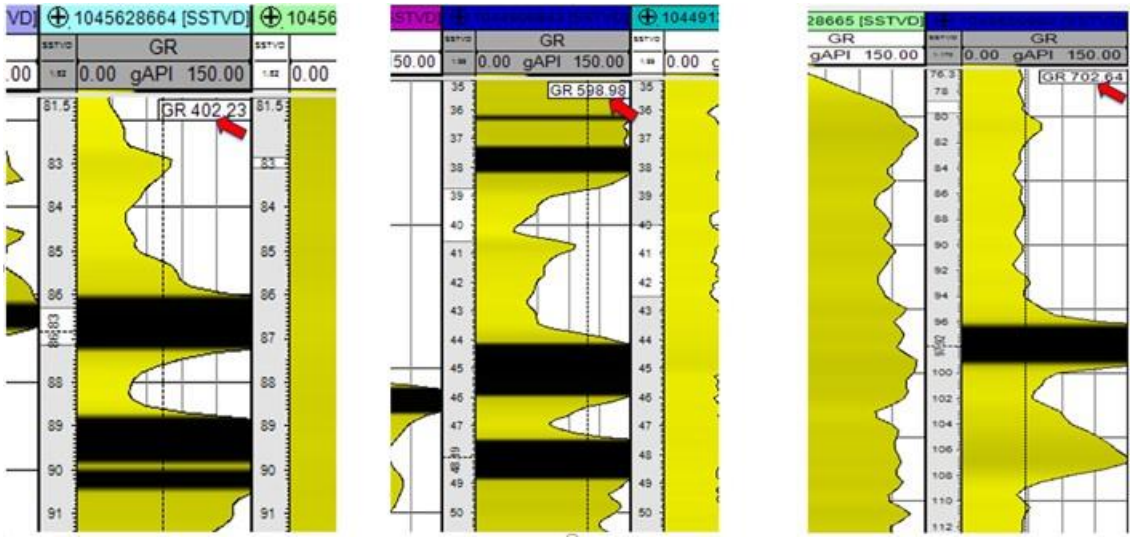

Figure 3.1: Gamma ray signatures showing high API values of black shales in the area.

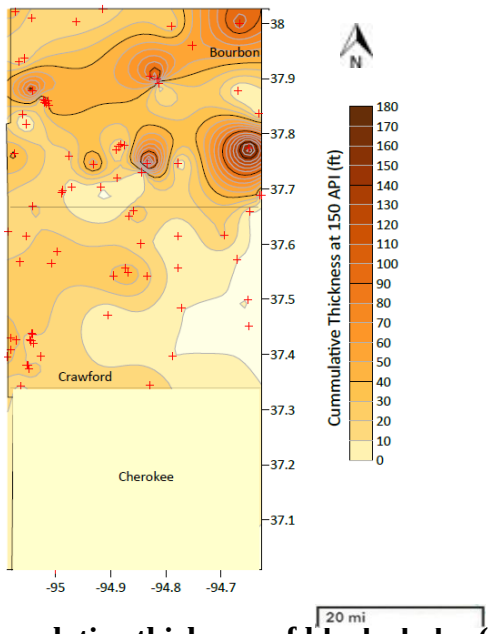

Figure 3.2: Isopach map of the cumulative thickness of black shales (within the top 300 ft of rock succession), based on gamma ray readings above 150 API.

The occurrence of black shales in subsurface is more prevalent in Bourbon County, Overall, the cumulative thickness of black shales decreases from northwest to southeast in the studied area, being absent in southeast Crawford County.

3.2 Groundwater Geochemistry

The temperature of the water samples measured in situ across the study area ranged from 13.5 °C to 24.8 °C, with an average value of 17.10 °C (Fig. 3.3a). pH values ranged from 6.27 to 7.96, with an average value of 7.11 (Fig. 3.3b). The conductivity ranged from 308.7 µS to 1433 µS, with an average value of 712.52 µS (Fig. 3.3c). The concentrations of dissolved oxygen ranged from 0.7 mg/L to 9.23 mg/L, with an average value of 3.53 mg/L (Fig. 3.3d). The alkalinity of the water samples ranged from 0.69 to 18.72 Meq/L, with an average of 4.81 Meq/L across the study area (Fig. 3.3e). Results for individual samples are provided in Appendix A.2.

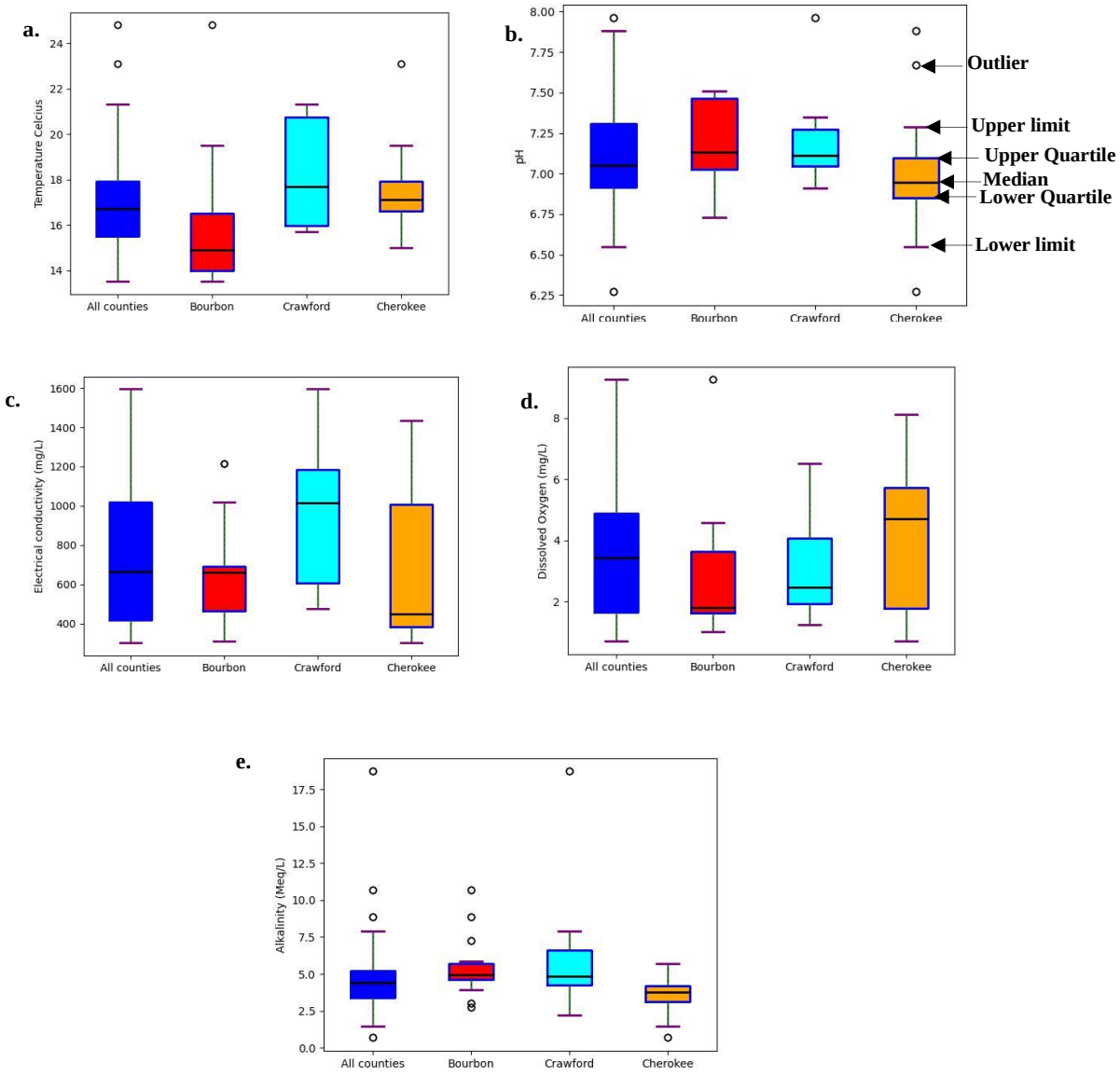

Figure 3.3: Distribution of (a) temperatures, (b) pH, (c) Electrical conductivity, (d)dissolved oxygen, and (e) alkalinity in the samples across the study area.

The concentrations of dissolved anions, including chloride (Cl^-), bromide (Br^-), sulfate (SO_4^{2-}), nitrate (NO_3^- as N), and nitrite (NO_2^- as N) averaged 41.58 mg/L, 0.13 mg/L, 71.75 mg/L, 2.66 mg/L, and 0.01 mg/L, respectively (Fig 3.4). Dissolved cation concentrations of sodium (Na^{+2}), ammonium (NH_4^+), potassium (K^+), magnesium (Mg^{+2}), calcium (Ca^{+2}), and strontium

(Sr^{+2}) averaged 46.84 mg/L, 0.76 mg/L, 8.20 mg/L, 12.72 mg/L, 85.07 mg/L, and 92.5 mg/L, respectively (Fig. 3.4). The concentrations of anions and cations in the samples was compared to the World Health Organization and the United States Environmental Protection Agency's (EPA) Maximum Contaminant Limit (MCL) for drinking water (Table. 3.1). Out of the forty-three (43) tested samples, one sample exceeded the MCL for Cl (with a maximum concentration of 300 mg/L), 4 samples exceeded the MCL for NO_3^- as N (with a maximum concentration of 32.85 mg/L), and 3 samples exceeded it for Sr (with a maximum concentration of 6.52 mg/L). Ion chromatography results for individual samples are provided in Appendix A.3 (anions) and A.4 (cations).

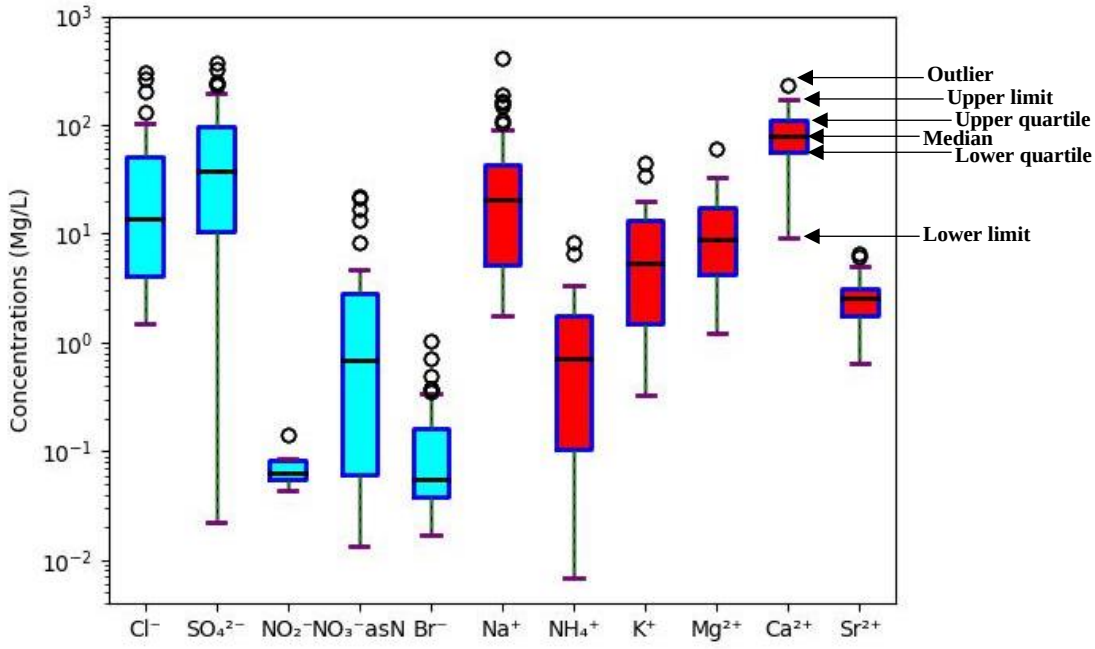

Figure 3.4: Anion (blue boxes) and cation (red boxes) concentrations in the water samples collected in the three studied counties. The plot excludes samples with a concentration of individual species below the limit of detection.

Table 3.1: WHO and EPA limits for anions and cations in drinking water, ("*" represents secondary limits, "-" represents no specified limit).

Species	WHO limit (mg/L)	EPA limit (mg/L)
Chloride	-	250*
Nitrite	3	1(as Nitrogen)
Nitrate	50	10 (as Nitrogen)
Sulphate	-	250*
Bromide	-	2 (children), 6 (Adult)
Phosphate	-	0.1
Strontium	4	4

An array of trace elements, besides uranium, were analyzed in the water samples, including lithium, barium, manganese, iron, copper, zinc, mercury, lead, nickel, cobalt, arsenic, selenium, molybdenum, and cadmium. Their average concentrations were 0.008 mg/L for U, 0.053 mg/L for Li, 0.063 mg/L for B, 0.20 mg/L for Mn, 0.57 mg/L for Fe, 0.004 mg/L for Cu, 0.018 mg/L for Zn, 0.001 mg/L for Hg, 0.001 mg/L for Pb, 0.002 mg/L for Ni, 0.0003 mg/L for Co, 0.001 mg/L for As, 0.001 mg/L for Se, 0.001 mg/L for Mo, and 0.00007 mg/L for Cd (Fig. 3.5). Trace element concentrations in the samples were also compared to EPA and WHO guidelines for drinking water (Table 3.2). Out of the 43 samples, one sample exceeded the EPA and/or WHO limit for U (max conc = 0.0365 mg/L), 6 samples exceeded the EPA and/or WHO limit for Fe (max conc = 11.17 mg/L), 6 samples exceeded the EPA and/or WHO limit for Hg (max conc = 0.016 mg/L), 18 samples exceeded the EPA and/or WHO limit for Mn (max conc = 3.3 mg/L). The results of trace metal analysis for individual samples are provided in Appendix A.5.

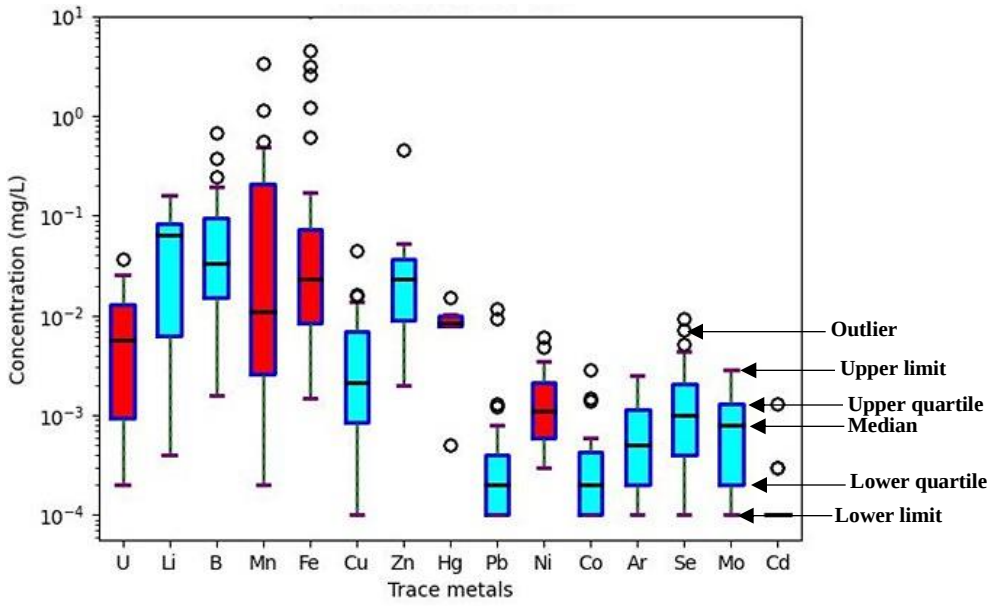

Figure 3.5: Trace metal concentrations in the water samples. Red boxes indicate metals with concentrations exceeding the EPA and/or WHO maximum contaminant limit for drinking water in at least one of the samples. The plot excludes samples with a concentration of individual species below the limit of detection.

Table 3.2: WHO and EPA limits for trace metals is drinking water ("*" represents secondary limits, "-" represents no specified limit).

Metals	WHO limit (ppm or mg/L)	EPA limit (ppm or mg/L)
Uranium	0.03	0.03
Boron	2.4	-
Manganese	0.08	0.05*
Iron	-	0.3*
Copper	2	1.0*
Zinc	-	5*
Mercury	0.006	0.002
Lead	0.01	0.015
Nickel	0.07	0.1
Arsenic	0.01	0.01
Selenium	0.04	0.05
Molybdenum	-	0.05
Cadmium	0.003	0.005

3.3 Geospatial Modeling

Two-dimensional geospatial modeling analysis of the major contaminants with concentrations above the EPA and/or WHO maximum contaminant limit revealed the distribution of the contaminants in the study area. The highest concentrations of Fe and Mn are found in Cherokee and Crawford Counties (Fig. 3.6), with the highest Fe concentrations in eastern Cherokee (Fig. 3.6a) and highest Mn concentrations in eastern Crawford County (Fig. 3.6b). Nitrate is high in southwest Bourbon and west Cherokee Counties (Fig. 3.7a). K is high in most of Bourbon County, and in isolated occurrences in east Crawford and central Cherokee Counties (Fig, 3.7b). The spatial distribution of chloride and electrical conductivity is similar, with the highest values for both in central Bourbon, eastern Crawford, and Western Cherokee Counties (Fig. 3.8). Uranium concentrations decreased from northwest to southeast in the study area, but only one sample in the west Cherokee County exceeded the safe limit (Fig. 3.9a). Very high mercury concentrations were found in extensive areas of Cherokee and Crawford Counties, with an isolated hot stop in western Bourbon County (Fig. 3.9b).

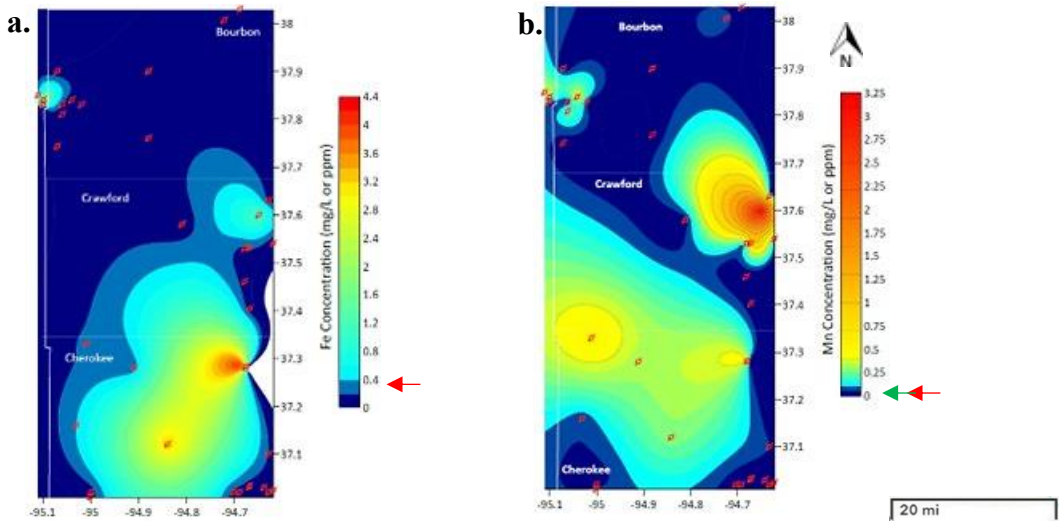

Figure 3.6: Spatial distribution of iron (a) and manganese (b) in the study area. The red arrow in the scale bar represents the U.S. EPA maximum contaminant limit for drinking water, and the green arrow, the WHO limit. Red dots on the map represent data points.

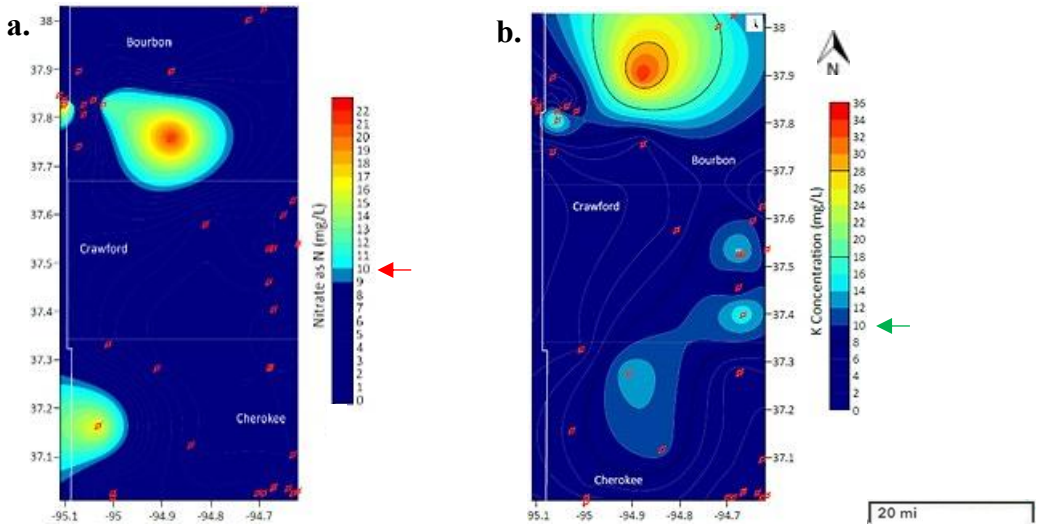

Figure 3.7: Spatial distribution of nitrate (a) and potassium (b) in the study area. The red arrow in the scale bar represents the U.S. EPA maximum contaminant limit for drinking water, and the green arrow, the WHO limit. Red dots on the map represent data points.

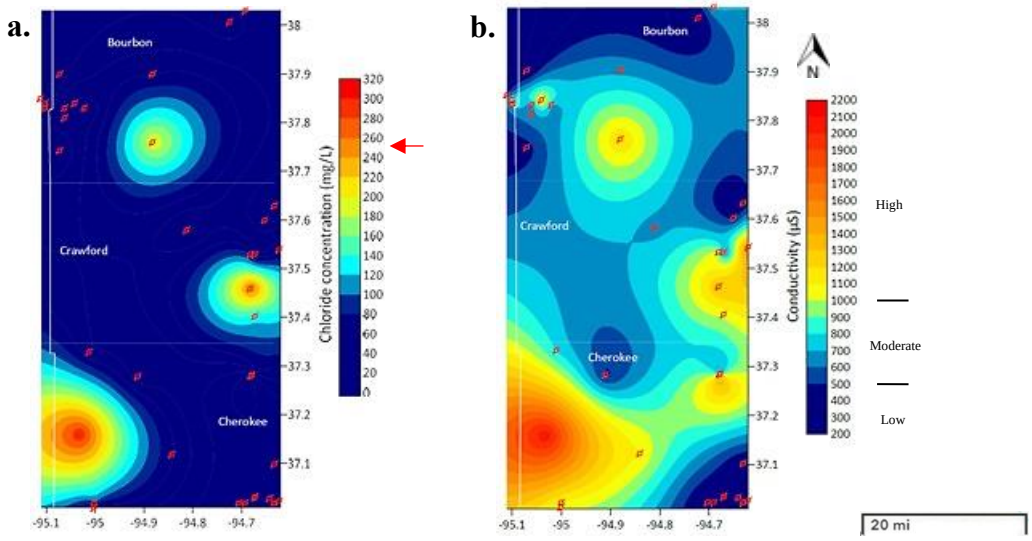

Figure 3.8: Spatial distribution of chloride (a) and electrical cond. (b) in the study area. The red arrow in the scale bar represents the U.S. EPA maximum contaminant limit for drinking water, and the green arrow, the WHO limit. Red dots on the map represent data points.

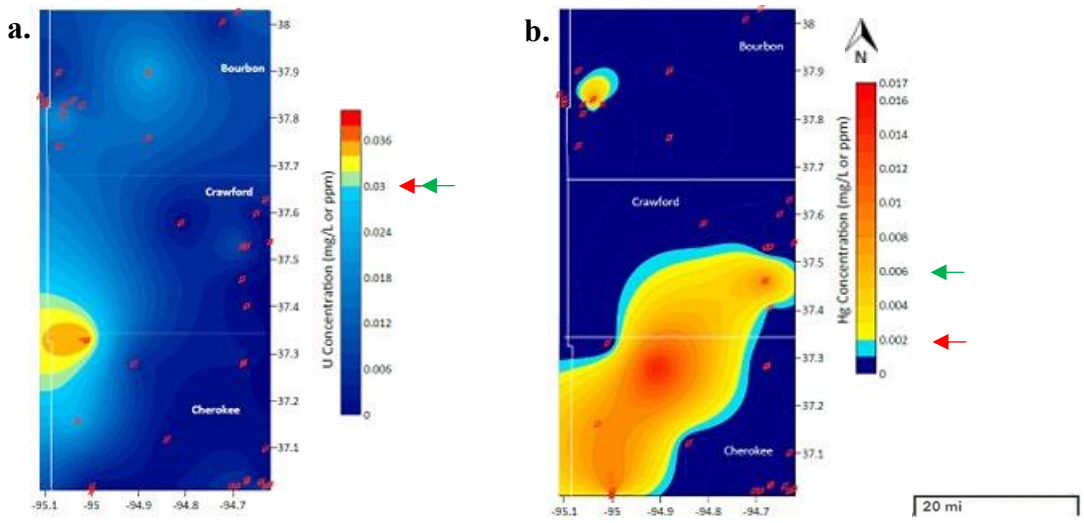

Figure 3.9: Spatial distribution of uranium (a) and mercury (b) in the study area. The red arrow in the scale bar represents the U.S. EPA maximum contaminant limit for drinking water, and the green arrow, the WHO limit. Red dots on the map represent data points.

3.4 Geochemical Modeling

Geochemical modeling was carried out to calculate some chemical and physical parameters, such as ionic strength, charge imbalance, water type, redox potential (Eh), etc., of the Ozark aquifer in the study area, based on the collected samples.

Ionic strengths ranged from 0.005 molal to 0.026 molal (making the B-dot equation suitable for our modeling). The charge imbalance error calculated for the samples all fell within the acceptable range of -5% to 5% (except for one sample, Bo-6e, which had a charge imbalance of -16%). The redox potentials ranged from 0.7358 V and 0.8176 V. Calculated Total Dissolved Solids ranged from 126 mg/L to 1729 mg/L (Fig. 3.11). The dominant water type for all three counties is Ca-HCO_3; other water types present in Crawford and Cherokee Counties include Na-HCO_3, Ca-Cl, Ca-SO_4, and Na-SO_4 (Fig. 3.10). Geochemical modeling results are provided in Appendix A.6.

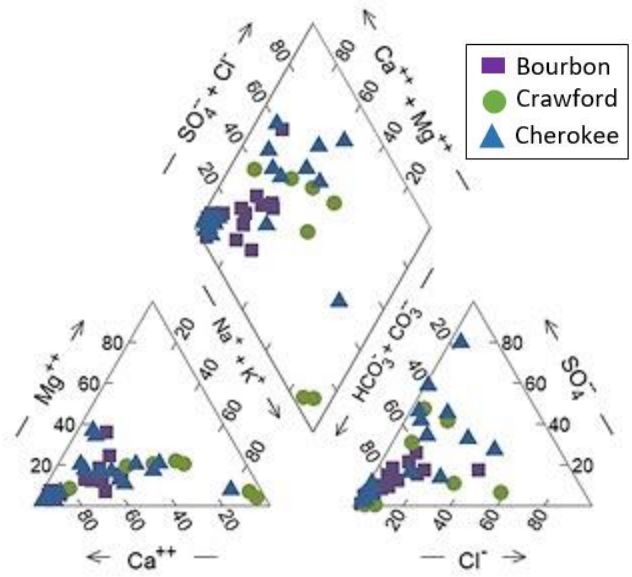

Figure 3.10: Piper diagram displaying the dominant ion species in the samples.

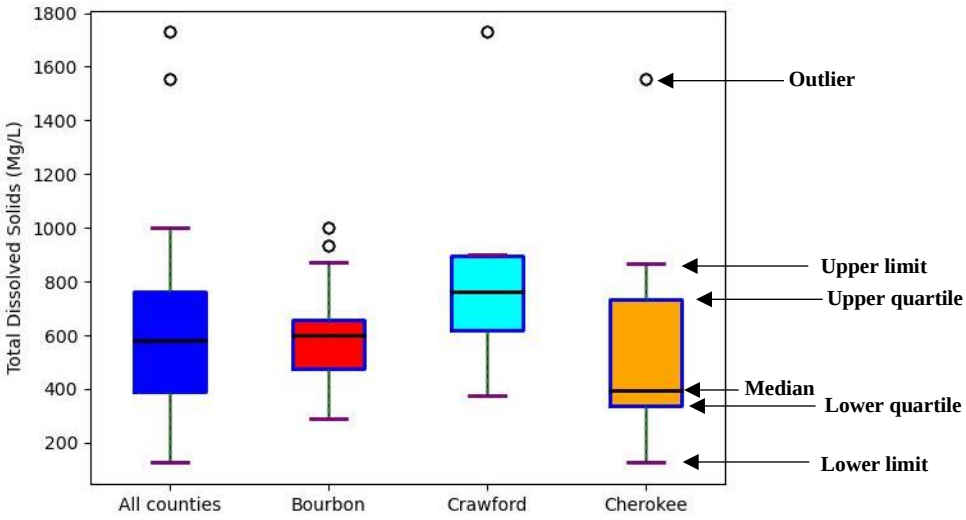

Figure 3.11: Distribution of Total Dissolved Solids in the samples across the study area.

3.5 Statistical Analysis

Spearman's rank correlation analysis was used to test the relationship between uranium and the variables controlling uranium mobilization (pH, alkalinity, Eh and dissolved oxygen) in the samples. The relationship between uranium concentrations and these variables revealed no

correlation with alkalinity (Fig. 3.11a, Table 3.3), a slight positive correlation with pH (Fig. 3.11b, Table 3.3), and a slight negative correlation with both Eh and dissolved oxygen (Fig. 3.11c-d, Table 3.3). Simple statistics are provided in Appendices A.7.

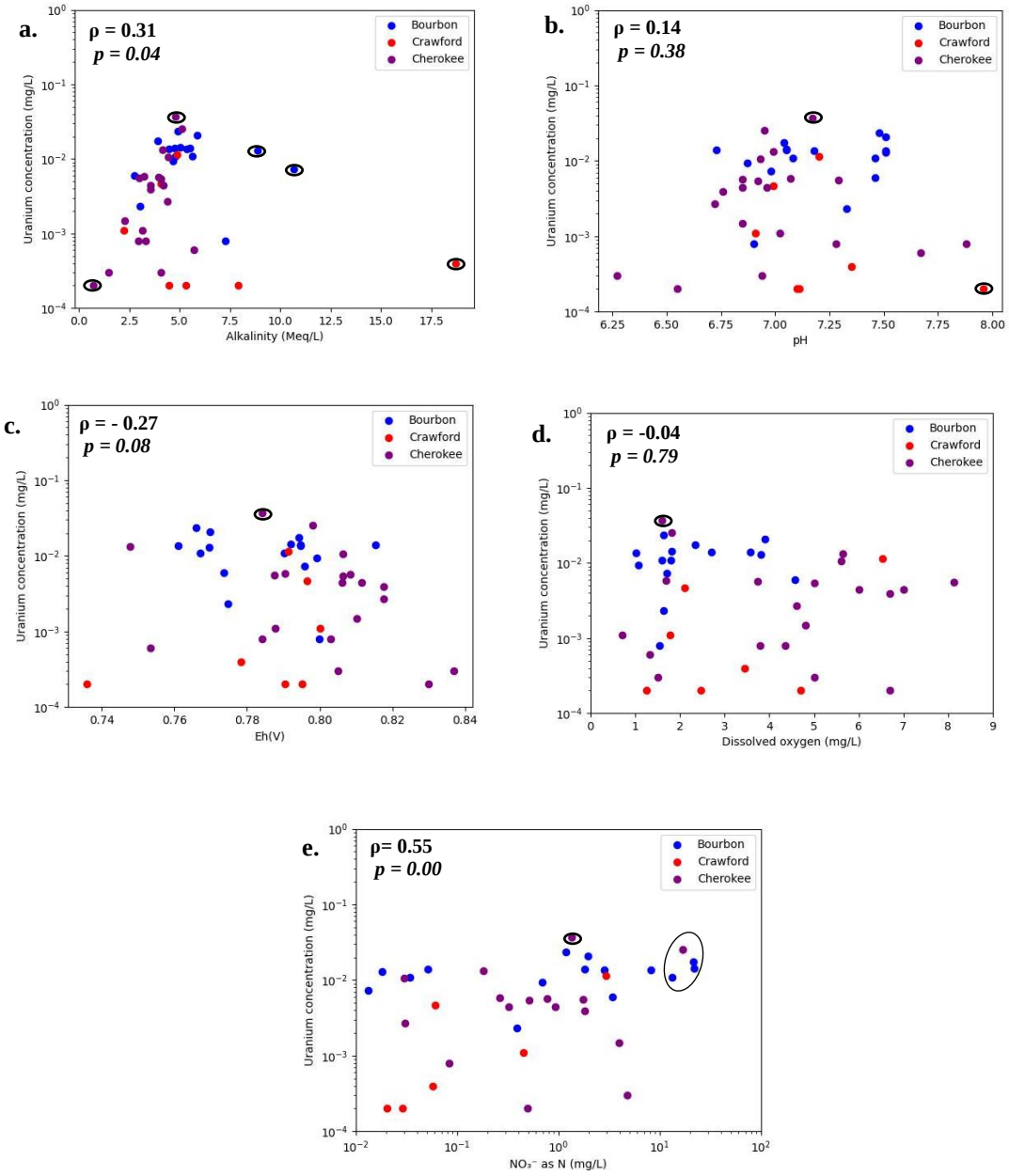

Figure 3.12: Scatter plots of uranium versus (a) alkalinity, (b) pH, (c) Eh, (d) dissolved oxygen and (e) Nitrate as N. Outliers are indicated by a black circle.

Table 3.3: Spearman's rank correlation coefficients between uranium concentration, Eh, pH, alkalinity, dissolved oxygen, and NO_3 as N (n=43, p-values are written below ρ -values).

	Alkalinity	pH	Eh	DO	NO_3 as N
U	0.31	0.14	-0.27	-0.04	0.55
	0.04	*0.38*	*0.08*	*0.79*	*0.00*

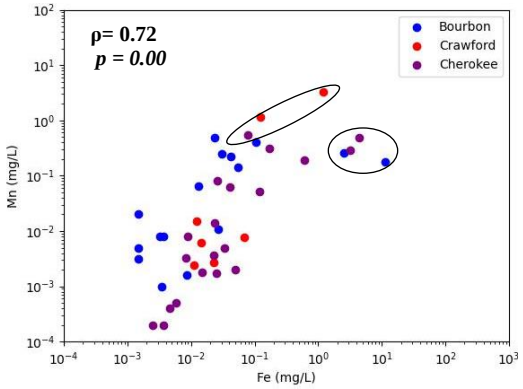

Figure 3.13: Cross plot of manganese versus iron concentrations in the samples. Outliers are indicated by a black circle.

3.6 Cancer Data

Certain chemical species, like uranium, mercury, iron, manganese, and nitrate, have been directly or indirectly linked to the development of some selected cancer types (Tchounwou *et al*., 2012; Ward *et al.*, 2018). For this reason, cancer incidence in the studied counties was compared to the entire state of Kansas and the United States over a 5-year period (2013-2017) (Table. 3.4). The data indicates that the incidence of kidney-related cancer per 100,000 people in the studied counties was higher than in the State of Kansas and the United States (Fig. 3.12), especially in Crawford and Cherokee Counties. Furthermore, the incidence of liver cancer per 100,000 people exceeds that of Kansas, and in Cherokee County, it exceeds the entire United States as well. The incidence of lung and bronchus cancer in Crawford and Cherokee Counties are higher than in the rest of the State of Kansas and the United States, and the incidence of brain and other nervous

system cancers in Bourbon and Crawford Counties (there is no data for Cherokee County) is about two times higher than in the rest of Kansas and the U.S. (Table 3.4 and Fig. 3.12).

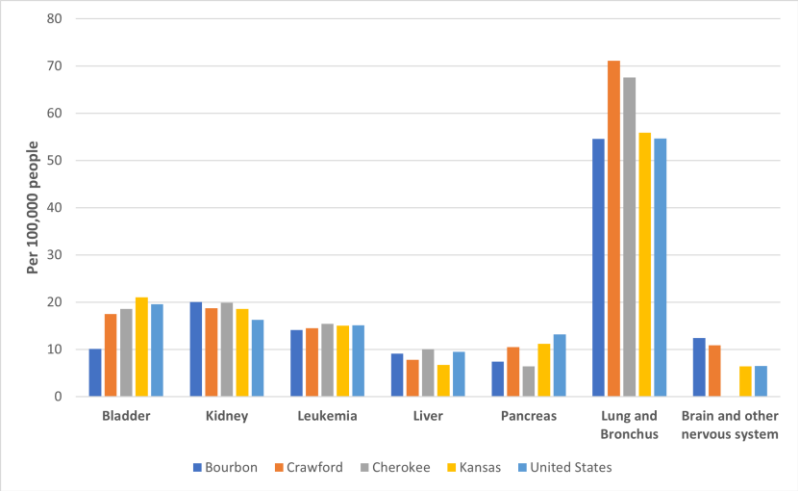

Figure 3.14: Age-adjusted cancer occurrence for selected cancer types per 100,000 population in the studied counties, State of Kansas, and the United States from 2013 -2017 (KDHE, 2023; NIH SEER, 2023). (Data on brain and other nervous systems for Cherokee County is suppressed.

Chapter 4 - Discussion

4.1 Relation Between Uranium Concentration and Groundwater Geochemistry

The pH and alkalinity values of the samples consistently fall within the same range across the study area (pH 6.27 – 7.96 and alkalinity 0.69 – 18.78 Meq/L). This regularity suggests a uniform geochemical environment. A scatter plot of the calculated $O_{2(aq)}$ activity and the measured pH of our samples overlaid on the redox-pH diagram below (Fig. 4.1) suggests that these samples lie in an oxidizing environment. According to the redox-pH diagram, the dominant aqueous uranium species within the range of $O_{2(aq)}$ activity and pH observed in our samples is $(UO_2)_2(CO_3)(OH)_3^-$ (oxidation state of uranium in this species is +6, an oxidized form).

Despite the fact that the redox state of the groundwater from the aquifer is oxic, our results do not necessarily describe the redox state of the shale units. The shale pore water may likely have a longer residence time than the water in adjacent aquifers, reflecting the lower permeabilities typical of shale. That, together with a relatively high availability of organic matter within the shales, may limit the extent to which they serve as a source of uranium to groundwater in the study area. Uranium concentrations in our samples also suggest that this element is not being mobilized into groundwater.

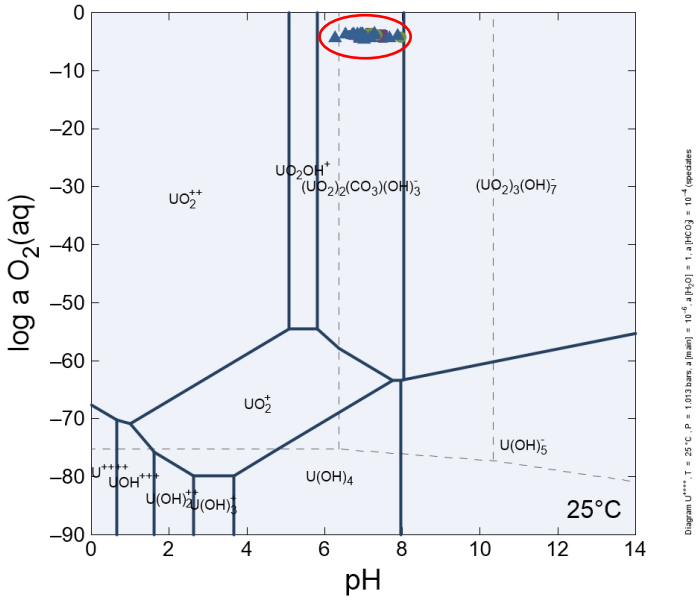

Figure 4.1: Redox pH diagram showing the dominant aqueous species of uranium at 25 °C. The red circle highlights the overlaid samples.

The presence of other contaminants, like nitrate, in the samples can influence the redox state of uranium, affecting its solubility and mobilization potential in an aqueous environment. Nitrates are formed by the oxidation of ammonium to nitrate (nitrification) with oxygen as the electron acceptor by aerobic microorganisms (USEPA, 2002; Kirk, 2023). The nitrification process is catalyzed by two genera of nitrite-oxidizing bacteria (Kirk, 2023) that can build organic molecules using energy obtained from inorganic sources, such as ammonia or nitrite (USEPA, 2002).

Nolan & Weber (2015) investigated the link between uranium contamination in major U.S. aquifers and the presence of nitrate. In their work, spatial correlation analysis of interpolated uranium and nitrate concentrations revealed a strong correlation ($r \geq 0.75$) within various regions throughout the High Plains and Central Valley aquifers. Testing the same relationship in our samples revealed a statistically significant strong correlation ($\rho \geq 0.55$). Nolan & Weber (2015) also reported mobilization of naturally occurring uranium in a shallow, fluvial aquifer in Germany, and both abiotic and biotic mechanisms, including nitrate-mediated mobilization, were suggested to control uranium solubility (Nolan *et al*., 2002; Nolan & Weber, 2015).

However, although nitrification, among other processes, may be contributing to uranium oxidation in the aquifer, the rate of oxidation and/or the amount of nitrate in the shale pore water may not be enough to oxidize and mobilize a significant amount of uranium from the black shales into the groundwater. Regardless, this should caution against the addition of nitrate to groundwater (e.g., from the indiscriminate use of fertilizers), which is a contaminant on its own but also could trigger a compound effect by releasing uranium into groundwater by oxidation.

Other factors that may contribute to oxidized uranium being trapped in the black shales or taken out of solution include adsorption, precipitation, and complexation. Oxidized uranium could be rapidly adsorbed onto mineral surfaces or organic matter in the aquifer, reducing its mobility. According to Wang *et al.* (2013), adsorption can mitigate the dissolved concentration and potential migration of uranium. Our samples were found to contain elevated concentrations of manganese. Near the Earth's surface, manganese is easily oxidized, giving rise to more than 30 known Mn oxides/hydroxide minerals (Post, 1999). Wang *et al. (*2013) showed that the mobility of U^{+6} can be retarded by the presence of Mn oxides via strong adsorption. Mn oxides have been recognized to be unfavorable for uranium remediation strategies that involve U^{+6} reduction because they can re-oxidize solid-phase U^{+4} products to soluble U^{+6} (Liu *et al.*, 2002; Fredrickson *et al.*, 2002; Wang *et al.*, 2013). According to Wang *et al.*, 2013, the biological cycling of Mn may jeopardize the stability of U^{+4} products even at low concentrations of Mn^{+2} and dissolved oxygen.

On the other hand, uranium could be precipitated out of solution due to changing geochemical conditions or reactions with other elements present in the aquifer, resulting in low concentrations in the groundwater. Valasco et al. (2021) investigated the interfacial reactions of U^{+6} in the presence of natural organic matter (NOM) at acidic and neutral pH. Their study revealed that the adsorption and precipitation of U^{+6} in the presence of NOM occur at pH 2 and pH 4, while the aqueous complexation of U by dissolved organic matter is favored at pH 7, preventing its precipitation.

The pH of our samples fell between 6 and 8, which does not support the absorption and precipitation of U^{+6} in the presence of NOM. Aqueous complexation of uranium by dissolved organic matter from the black shales seems plausible; however, this will prevent uranium from precipitating out of solution (Valasco et al., 2021). Therefore, the adsorption of uranium in the

presence of Mn oxides may be a plausible explanation for why we have a low concentration of uranium in our samples despite the oxidizing conditions, considering the elevated concentrations of manganese found in our samples. If that is the case, then Mn^{+2} oxidation and in situ formation of Mn oxides may serve as a potential remediation strategy for regions with high concentrations of uranium in groundwater (Wang *et al.,* 2013) since Mn oxides are highly chemically active and strong scavengers of heavy metals (Post *et al.*, 1999).

4.2 Relation Between Lithology and Uranium in Water

One of the key findings of this study is that the presence of uranium in the groundwater, except in one well in northwestern Cherokee County, falls within the established safety limits set by the EPA and the WHO for drinking water (Fig. 3.9a). This compliance with regulatory standards for most wells is reassuring from a public health perspective, indicating that the groundwater in the study area is safe for consumption with respect to uranium contamination.

It is possible that the lack of widespread uranium concentration above the EPA and WHO limits in the area may be due to the prevailing adsorption of mobile U^{+6} by MnO_2 in the aquifer. Therefore, the process of adsorption within the aquifer in our study area is a crucial factor in keeping uranium out of solution, thereby not making uranium a contaminant of concern in the groundwater.

4.3 Source of Contaminants

The analysis of groundwater samples from our study area revealed the presence of several contaminants, including nitrate, manganese, iron, and mercury. The established limits set by the EPA and the WHO serve as benchmarks for water quality, establishing critical parameters for assessing the suitability of groundwater for drinking purposes.

The elevated concentrations of these contaminants could be attributed to a combination of natural processes and anthropogenic activities. The geological characteristics of the study area may influence the leaching of certain elements into the groundwater, whereas agricultural runoff, industrial discharges, and other human activities could contribute to the contamination.

Nitrate

Nitrate levels in well water are often significantly higher than those in surface water (WHO, 2017). Nitrate can reach groundwater as a consequence of agricultural activities (including excess application of inorganic nitrogenous fertilizers and manures), erosion of natural deposits (such as organic coal, shale, and marine mudstone), waste-water disposal, oxidation of nitrogenous waste products in human and other animal excreta, including septic tanks (USEPA, 2009; WHO, 2017), and the nitrification of nitrate and/or ammonia by nitrifying bacteria (USEPA, 2002). According to the Minnesota Department of Health, shallow wells, wells dug into sand aquifers, and wells with damaged or leaking casings or fittings are the most vulnerable to nitrate contamination. Given that samples with elevated nitrate concentrations were all collected from wells with a depth of less than 7 meters, nitrate is likely to be derived from surficial sources. Three of the four wells contaminated by nitrate were located in the Bourbon Country, the most rural and agriculturally dense of the three countries. Hence, the high nitrate concentration is possible due to a combination of sources, including nitrogen-based fertilizers, manure, and other animal and human wastes.

Iron and Manganese

Iron and manganese occur naturally in soil and rocks and are introduced into groundwater as a result of the oxidation of these geologic materials (Ochieng *et al.*, 2010). Iron and manganese are similar in terms of occurrence, sensitivity to redox conditions, and oxidation states. Differences

in behavior are largely attributed to Fe^{2+} oxidizing more rapidly than Mn^{2+} (Davison, 1993). Although manganese occurs naturally in many surfaces and groundwater, anthropogenic sources can also contribute to high levels of manganese in groundwater (WHO, 2017). Anthropogenic sources include industrial effluents (Rudi *et al.*, 2020), sewage leakage (Lü *et al*., 2022), land fill leachate, and mining.

Mine waste is a source of toxic metal leachates resulting in acid-mine drainage. Common in areas known for coal mining (such as Bourbon, Crawford, and Cherokee Counties), acid-mine drainage is the result of tailings and overburden being exposed to air and water (Prasad *et al.*, 2016). This oxidation process occurs in undisturbed rocks but at a slow rate, and the water is able to buffer the acid generated (Ochieng *et al.*, 2010). Mining, however, increases the exposed surface area of these rocks, thereby accelerating the process beyond the water's natural buffering capacity (Jennings et al., 2008; Prasad *et al.*, 2016). Acid-mine drainage has been identified as the largest source of environmental problems caused by the mining industry (Prasad *et al.*, 2016).

Under natural conditions, the redox behavior of iron and manganese is the opposite of uranium. While uranium is insoluble under oxidizing conditions, both Fe and Mn are mobilized into solution under reducing conditions (Davison, 1993; Dvorak *et al.,* 2021), existing in the solid form, often as very small particles (colloids), in oxidizing settings (Dvorak *et al.*, 2021). The close relationship between iron and manganese concentrations in our samples is shown in (figure. 4.3). The correlation ($\rho = 0.72$) might hint at a possible common source.

The presence of organic matter also impacts the mobility of iron and manganese (Zhang *et al.*, 2020) due to the influence of the former in the reduction of iron and manganese. Environments with abundant organic matter can lead to the reduction and mobilization of iron and manganese

into groundwater (Hem, 1995; Lane *et al*., 1999; Neidhardt *et al*., 2014; Zhang *et al.*, 2020; Lü *et al*., 2022), fostered by the combination of fine-grained sediments (Nickson *et al.*, 2000; Zhang *et al.*, 2020) and most likely, microbial reactions (Chapelle & Lovley, 1992).

However, both metals are more abundant in Cherokee and eastern Crawford Counties, closer to the Tri-State Mining District, which signals the possibility of mine waste contribution. The distribution of Fe concentrations also coincides closely with the distribution of mercury, discussed below.

Mercury

Mercury exists naturally and as a man-made contaminant in the environment (Rice *et al.*, 2014). According to the U.S. Geological Survey, mercury is emitted by natural sources, such as volcanoes, geothermal springs, geologic deposits (such as coal), and the ocean. Human related sources primarily include coal combustion (accounting for one-third of the total atmospheric mercury contribution in the U.S.) (CSWRCB, 2017; USGS, 2019), industrial operations (including effluents and emissions), waste incineration, and mining. Mercury contamination is global and affects many waters, including those with no obvious mercury source because mercury emissions generally disperse widely in the atmosphere before being deposited to the earth (USGS, 2019). Atmospheric mercury can react with other elements and precipitate onto the earth's surface (CSWRCB, 2017), either as wet deposition (rain or snow) or as dry deposition (gas phase or particulate deposition to surfaces during precipitation-free periods) (Wentz et al., 2014), eventually finding its way into the groundwater by infiltration.

The behavior of mercury in groundwater with respect to redox chemistry is complex and depends on various factors, such as the forms of mercury, redox conditions, and the presence of

other substances (Alexandra *et al.*, 2022). In an oxidizing environment, elemental mercury (Hg^0) tends to remain in a gaseous form that is less soluble in water (Ravichandran, 2004). Under these conditions, elemental mercury can, however, undergo slow oxidation to divalent mercury (Hg^{+2}), which can form complexes with organic and inorganic ligands or adsorb to particles, reducing its mobility in water (Bloom & Crecelius, 1983; King e*t al.*, 2000). In reducing environments, such as anaerobic sediments or groundwater with low oxygen levels, divalent mercury (Hg^{+2}) can be microbially reduced back to elemental mercury (Hg^0), a more volatile form that that can be released into the atmosphere or reoxidized under oxidizing conditions (Gilmour *et.al.*, 1992). Furthermore, Hg^0, under certain conditions, may be transformed into methylmercury (MeHg) through microbial methylation processes (Morel & Kraepiel, 1998; Heyes *et al.*, 2006; Hu *et al.*, 2013; WHO, 2017). Methyl mercury is more mobile and can bioaccumulate in organisms (Driscol *et al.*, 2013).

According to the California State Water Resource Control Board, most mercury deposited from the atmosphere will re-volatize or adsorb organic material in the soil; as a result, only a very small amount of mercury is transported to groundwater. Elevated mercury in groundwater may result from releases from past mining and chemical spills or from improper disposal of materials that contain mercury.

The distribution of Hg (coincident with Fe), showing the highest concentrations in Cherokee and eastern Crawford Counties, associated with the long history of coal mining in Cherokee County and the Tri-State Mining District, provides a plausible explanation for the presence of mercury in the samples in orders of magnitudes above the EPA and WHO limits for drinking water.

Potassium

Potassium can be introduced into groundwater through natural weathering of silicate rocks. However, elevated amounts of potassium can be introduced into groundwater as a result of anthropogenic activities, such as the excessive use of fertilizers for agricultural purposes and the breakdown of animal or waste products. (Saha *et al.*, 2019).

4.4 Potential Health Risk of Contaminants Found in the Study Area

Concentrations of Total Dissolved Solids exceeded the EPA primary limit (500 mg/l) in 24 of our samples. The Exceedances of the EPA and WHO limits for nitrate, manganese, iron and mercury raise concerns about potential health risks associated with drinking water from these wells. High nitrate levels are associated with shortness of breath, methemoglobinemia (blue-baby syndrome), and gastrointestinal infection, particularly in bottle-fed infants (WHO, 2017; USEPA, 2024) and pregnant individuals (WSDH, 2022). Epidemiologic studies have been carried out to evaluate the relationship between drinking water nitrate and cancer, adverse reproductive outcomes, or thyroid disease. Considering all studies to date, the strongest evidence for a relationship between drinking water nitrate ingestion and adverse health outcomes (besides methemoglobinemia) is for colorectal cancer, thyroid disease, and neural tube effects (Ward *et al.*, 2018).

According to Ward *et al.* (2018), four of the five published studies of colorectal cancer found evidence of an increased risk of colorectal or colon cancer associated with water nitrate levels that were mostly below the respective regulatory limits (De Roos *et al.*, 2003; McElroy *et al*., 2008; Espejo-Herrera *et al.*, 2016; Schullehner *et al.*, 2018). Populations with the highest exposure to nitrate from their drinking water are those living in agricultural regions, especially

those drinking water from shallow wells near nitrogen sources (e.g., crop fields, animal feeding operations, etc.) (Ward *et al.*, 2018).

According to the EPA, the nitrification process of ammonia or nitrite to nitrate also leads to the formation of disinfectant by-products (DBPs). The U.S. Center for Disease Control and Prevention states that chronic exposure to DBPs may increase the risk of cancer. Humans exposed to unusually large amounts of DBPs could experience liver damage and decreased nervous activity.

Manganese is an essential nutrient for the human body (WHO, 2017); however, excessive exposure to high levels of manganese in drinking water can lead to adverse health effects. According to the WHO, the primary concern for manganese toxicity in mammals (including humans) is the central nervous system. In addition to neurotoxicity, renal injury is another adverse effect associated with manganese intoxication (Niknahad *et al*.,2020); and because manganese is absorbed and excreted by the liver, it is a target organ for toxicity and can therefore damage the liver (USEPA, 2009).

Like manganese, iron is also an essential element in human nutrition (WHO, 2017). There is no prescribed limit for iron concentration in drinking water by the WHO, except for a secondary maximum contaminant limit set by the EPA. However, several adverse health conditions are linked to elevated intake of iron into the body, the most common being hemochromatosis (also called bronze diabetes), a disorder in which extra iron builds up in the body to harmful levels and in turn, causes multiple organ dysfunction (Porter & Rawla, 2023). In contrast to other metals, such as arsenic, chromium, nickel, etc., iron does not have carcinogenic properties per se; nevertheless, iron overload is clearly associated with a high risk for carcinogenesis (Huang, 2003; Papanikolaou & Pantopoulos, 2005). According to Anderson (2007), the liver and heart are the major targets of

damage induced by reactive iron species in the body, but other organs such as the pancreas, thyroid, joints, skin, gonads, pituitary, and endocrine organs are also sensitive to the toxic effects of iron (Anderson *et al*., 2001; O'Nail & Powell, 2005; Porter & Rawla, 2023). The liver is the major iron storage in the body, and it is not surprising that hepatoxicity is a major consequence of body iron loading (Ramm & Ruddell, 2005).

Mercury is ranked third of the most toxic elements to human health by the United States Government Agency for Toxic Substances and Disease Registry (Budnik & Castelyn, 2019). According to the World Health Organization, the toxic effects of inorganic mercury compounds are seen mainly in the kidneys in both humans and laboratory animals following long-term exposure. In humans, acute oral poisoning results primarily in hemorrhagic gastritis and colitis; however, the overall damage is to the kidney. The overall weight of evidence is that mercury (II) chloride has the potential to increase the incidence of some benign tumors at sites where tissue damage is apparent (WHO, 2017).

Inorganic mercury can be transformed into more toxic methylmercury by biotic and abiotic means (Hu *et al.*, 2013; WHO, 2017). Mercury has profound cellular, cardiovascular, hematological, pulmonary, renal, immunological, neurological, endocrinal, reproductive and embryonic toxicological effects (Rice *et. al.*, 2014). Exposure to mercury can lead to serious damage to the lungs, kidney, central nervous system, and impaired neurological development in infants and children (Freire *et al.*, 2010; Rice *et. al.*, 2014).

No limits have been set by the regulatory bodies for potassium in drinking water; however, potassium has been directly and indirectly linked with a number of health concerns due to excessive accumulation in the body. The WHO has described potassium as an essential element in

humans and is seldom, if ever, found in drinking water at levels that could be of concern for healthy humans. Where potassium permanganate is used in municipal water treatment, concentrations of added potassium can be up to a maximum of 10 mg/L (WHO, 2009). This raises concern considering the concentrations of potassium found in our samples are up to about 36 mg/L, especially in the Bourbon County. Potassium intoxication is rare, because potassium is rapidly excreted in the absence of pre-existing kidney damage (Gosselin *et al*., 1984; WHO, 2009). Excessive potassium is a health concern only for individuals in high-risk groups (i.e. with kidney dysfunction or other diseases, such as heart disease, coronary artery disease, hypertension, diabetes, adrenal insufficiency, pre-existing hyperkalemia; people taking medications that interfere with normal potassium-dependent functions in the body; and older individuals or infants) (WHO, 2009).

4.5 Relation Between Contaminants and Cancer

The study has unveiled the presence of groundwater contaminants (specifically manganese, iron, mercury, and nitrate) and high incidence of various types of cancer in the studied counties. However, a significant correlation between these contaminants and cancer cases could not be firmly established due to the lack of detailed cancer data. Nonetheless, these findings warrant the need for a closer look at this potential connection. Notably, the kidney and liver appear to be particularly susceptible organs to the impact of these carcinogenic substances, what could explain the high incidence of liver and kidney cancers in the studied counties.

Two public water supply wells serving over 2000 homes each were sampled in this study. One of them exhibited mercury concentration far surpassing both EPA and WHO guidelines for drinking water (0.002 mg/L and 0.006 mg/L respectively), raising concerns about the toxic effect

on the consumers. The U.S. Center for Disease Control and Prevention also states that people are exposed to disinfection by-products (DBPs) by drinking chlorinated and brominated water. DBPs are formed when disinfectants like chlorine interact with natural organic materials in water (nitrate, nitrite, ammonium, and ammonia). This raises a potential health concern since chlorination is a common practice in public water treatment facilities (as seen in Crawford County). In the western part of Crawford County (where these two water treatment plants are located) and the eastern part of Cherokee County, the samples show elevated chloride, bromide, ammonium, and nitrate concentrations.

Disturbingly, Cherokee County stood out with elevated mercury, iron, and manganese contamination and high incidence rates (per 100,000 persons) of leukemia, bladder, kidney, liver, and lung and bronchus cancers. These contaminants (Hg, Fe and Mn) are directly linked to the development of these cancer types, which suggests a connection between these cancers and the contaminants found in groundwater.

Crawford County shows a high incidence of bladder, pancreas, lung and bronchus, and brain and nervous system cancers, and the groundwater is equally contaminated by mercury, iron, and manganese.

Bourbon County displays a high incidence of kidney, liver, and brain (and nervous system) cancers. Crawford County takes the lead in the occurrence of lung and bronchus cancer. Interestingly, Bourbon County, characterized by elevated nitrate concentrations in wells, also ranks highest in the incidence of brain and nervous system cancer, but the main contaminant found in this county is nitrate. High concentrations of mercury, iron, and manganese are found locally, particularly in the central-west part of the county. This is relevant because anecdotal data provided

by some residents point to the high incidence of cancer among young adults in the Uniontown area, located in central-west Bourbon County. The elevated nitrate concentrations found in well water in Bourbon County may have contributed to the high incidence of brain (and nervous system) cancer since nitrate has been linked to neural tube effects.

These findings underscore the critical importance of addressing and mitigating groundwater contamination to safeguard public health. To establish a more direct link between groundwater contamination, cancer, and public health, however, more detailed, integrative studies that include medical data would have to be performed in the area.

4.6 Measures to Mitigate Contaminants in Water

Nitrate

The U.S Environmental Protection Agencies recommends several effective nitrate treatments technologies for drinking water including ion exchange, reverse osmosis, and electrodialysis. Ion exchange resins are like tiny magnets that attract and hold the nitrate from passing through the water treatment system. Reverse osmosis is a water purification method that forces the nitrate contaminated water through a semi-permeable membrane that retains nitrate. Electrodialysis uses a direct electric current to migrate ions through membranes, where the nitrate is then trapped (USEPA, 2021). In addition, domestic wells should be constructed in a safe spot (away from nitrate sources like septic systems, fertilizers, and animal wastes) and regularly inspected for damage.

Iron

Effectively treating iron depends on the form(s) of iron present, the chemistry of the water, and the type of well and water system (Minnesota Department of Health, 2023). The various forms

of iron present in drinking water include ferrous iron (the water comes out of the faucet clear, but turns red or brown after standing), ferric ion (water is red or yellow when it first comes out of the faucet), and organic iron (the water is usually yellow or brown but may be colorless) (Minnesota Department of Health, 2023). The Minnesota Department of Health recommends the use of water softeners and iron filters for treating ferrous iron. Ferric iron can be treated using an iron filter, aeration, sediment filter, carbon filter, or water softener. For organic iron, chemical oxidation followed by filtration is recommended.

Manganese

The EPA recommends several effective treatment technologies available for manganese removal in drinking water, including catalytic precipitation (typically by greensand with permanganate or chlorine backwashes), oxidation and filtration (e.g., with ozone or permanganate to form particulates, and then physical removal by filtration with low-pressure membranes or lime softening), and biological treatment.

Mercury

According to the EPA, conventional chemical coagulation, sedimentation, and filtration can remove up to 80% of inorganic mercury, but only 20-40% of organic mercury. Ferric sulfate is more effective than aluminum sulfate, and it works better in the presence of high concentrations of suspended solids. Powdered activated carbon is effective at removing inorganic and organic mercury and can be used to improve removal during coagulation. Granular activated carbon treatment is also useful (USEPA, 2021). However, ion exchange may be an alternative method (Chiarle et al., 2000).

Generally, detecting contaminants in drinking water is challenging as they are often tasteless, odorless, and invisible. The World Health Organization (WHO) and the Environmental Protection Agency (EPA) advocate for regular testing of drinking water sources, such as wells, to identify contaminants early. Public awareness is crucial, emphasizing water conservation, proper disposal practices, and the protection of drinking water sources. Additionally, regulatory authorities play a vital role by providing and enforcing strict legislatures to control the discharge of contaminants into water bodies by industries.

The collaboration among regulatory bodies, individuals, communities, and industries is essential for effective prevention and reduction of water contamination, ultimately contributing to improved public health and well-being. Public water supply facilities are advised to conduct annual testing of wells for trace metal contamination as part of their commitment to water quality assurance.

Chapter 5 - Conclusions

The analysis of groundwater samples from the study area did not show high uranium concentration but revealed the presence of several other contaminants, including nitrate, manganese, and mercury, with concentrations exceeding the EPA and WHO limits for drinking water, thereby making the groundwater in most of the area unfit for drinking in its natural state. The study highlighted significant correlations between these contaminants and various types of cancer, particularly affecting the kidney, liver, pancreas, lung and bronchus, blood, brain and nervous system.

The absorption of uranium by Mn oxides in the aquifer may have played a crucial role in removing mobilized uranium from groundwater in the aquifer, making it generally compliant with regulatory standards. While manganese may be a contaminant in the study area, it may have also played a crucial role in adsorbing uranium out of the groundwater. Nitrate concentrations in the samples influenced the redox state of uranium, potentially affecting solubility, but the rate of oxidation and/or the amount of nitrate in the shale pore water might not be sufficient to overcome the absorption rate for significant mobilization, resulting in uranium concentration generally complying with safety standards.

Nitrate contamination is linked to agricultural activities, while manganese, iron and mercury have natural and anthropogenic sources (industrial discharge and past mining activities). Mercury ranked among the most toxic elements found in the study area, posing severe health risks, including kidney damage and neurological effects.

Various treatment technologies prescribed by the EPA and the WHO for nitrate, iron, manganese, and mercury removal have been highlighted. The importance of routine well testing,

public awareness, and proper disposal practices cannot be over-emphasized. These are crucial preventive measures for conserving drinking water sources.

In conclusion, this study underscores the urgent need for mitigation strategies to address groundwater contamination to safeguard public health. The findings emphasize the complex interplay between geochemical, geological, and anthropogenic factors influencing groundwater quality, necessitating comprehensive measures to ensure safe drinking water and prevent adverse health effects. Collaboration among regulatory bodies, communities, academic institutions, and industries is vital for the effective prevention and reduction of groundwater contamination. Water treatment facilities are recommended to conduct regular testing of wells for trace metal contamination to improve water quality assurance.

References

Adler, H. H., (1974). Concept of uranium-ore formation in reducing environments in sandstone and other sediments. In Formation of uranium deposits, Proceedings of a Symposium; Athens, May 6-10, 1974; International Atomic Energy Agency: Vienna.

Alexandra E. Spyropoulou, Yannis G. Lazarou, Andreas A. Sapalidis, Chrysi S. Laspidou, Geochemical modeling of mercury in coastal groundwater, Chemosphere, Volume 286, Part 1, 2022, 131609, ISSN 0045-6535, https://doi.org/10.1016/j.chemosphere.2021.131609.

Anderson G. J. (2007). Mechanisms of iron loading and toxicity. *American journal of hematology*, *82*(12 Suppl), 1128–1131. https://doi.org/10.1002/ajh.21075.

Anderson, L. J., Holden, S., Davis, B., Prescott, E., Charrier, C. C., Bunce, N. H., ... & Pennell, D. J. (2001). Cardiovascular T2-star (T2*) magnetic resonance for the early diagnosis of myocardial iron overload. *European heart journal*, *22*(23), 2171-2179.

Alam M. S., Cheng T., (2014). Uranium release from sediment to groundwater: influence of water chemistry and insights into release mechanisms. J Contam Hydrol. 2014 Aug; 164:72-87. doi: 10.1016/j.jconhyd.2014.06.001. Epub Jun 6. PMID: 24954631.

Baják P., Csondor K, Pedretti D., Muniruzzaman M., Surbeck H., Izsák B., Vargha M., Horváth Á., Pándics T., Erőss A., (2022). Refining the conceptual model for radionuclide mobility in groundwater in the vicinity of a Hungarian granitic complex using geochemical modeling, Applied Geochemistry, Volume 137, 105201, ISSN 0883-2927, https://doi.org/10.1016/j.apgeochem.2022.105201.

Balaram V., Rani A., Rathore D. P. S., (2022). Uranium in groundwater in parts of India and world: A comprehensive review of sources, impact to the environment and human health, analytical techniques, and mitigation technologies, Geosystems and Geoenvironment, Volume 1, Issue 2, 2022, 100043, ISSN 2772-8838, https://doi.org/10.1016/j.geogeo.2022.100043.

Bell, E. L., and Fortner, J. R., 1981. Soil survey of Bourbon County, Kansas: U.S. Department of Agriculture, Soil Conservation Service and Kansas Agricultural Experiment Station, 89 p., 50 maps.

Bloom, N. S., & Crecelius, E. A., (1983). Factors affecting the solubility of mercuric sulfide in natural waters. Journal of Environmental Science & Technology. DOI:10.1021/es00118a004.

Bonotto, D. M., Wijesiri B., Goonetilleke A., (2019). Nitrate-dependent Uranium mobilization in groundwater, Science of The Total Environment, Volume 693, 133655, ISSN 0048-9697, https://doi.org/10.1016/j.scitotenv.2019.133655.

Bradford, G. R., and Amrhein, C., (1993). Uranium and other trace elements in algae growing in drainage and evaporation pond waters in the San Joaquin Valley. UC Salinity/Drainage Program Annual Report, 1991–1992. Division of Agriculture and Natural Resources, University of California, Riverside, CA. pp. 118–123.

Brown, C. J., Walter, D. A., Colabufo, S., (1999). *Iron in the Aquifer System of Suffolk County, New York, 1990–1998*; Water Science Center U.S. Geological Survey: New York, NY, USA.

Brindha, K., & Elango, L., (2013). Occurrence of uranium in groundwater of a shallow granitic aquifer and its suitability for domestic use in southern India. *Journal of Radioanalytical and Nuclear Chemistry*, *295*(1).

Budnik, L. T., Casteleyn, L., (2019) Mercury pollution in modern times and its socio-medical consequences, Science of The Total Environment, Volume 654, 2019, Pages 720-734, ISSN 0048-9697, https://doi.org/10.1016/j.scitotenv.2018.10.408.

California State Water Resource Control Board, (2017). Groundwater Information Sheet: Mercury. Web accessed; [14th January 2024], chrome-extension://efaidnbmnnnibpcajpcglclefindmkaj/https://www.waterboards.ca.gov/gama/docs/coc_mercury.pdf.

Chapelle, F. H. & Lovley, D. R., (1992). Competitive Exclusion of Sulfate Reduction by Fe (III)-Reducing Bacteria; A Mechanism for Producing Discrete Zones of High-Iron Ground Water, GROUND WATER, Vol. 30, No. 1, January-February 1992.

Chiarle, S., Ratto, M., Rovatti, M., (2000). Mercury removal from water by ion exchange resins adsorption, Water Research, Volume 34, Issue 11, 2000, Pages 2971-2978, ISSN 0043-1354, https://doi.org/10.1016/S0043-1354(00)00044-0.

Cumberland S. A., Douglas G., Grice K., & Moreau J. W., (2016). Uranium mobility in organic matter-rich sediments: A review of geological and geochemical processes, Earth-Science Reviews, Volume 159, Pages 160–185, ISSN 0012-8252.

Davison, W., (1993). Iron and manganese in lakes, Earth-Science Reviews, Volume 34, Issue 2, Pages 119-163, ISSN 0012-8252, https://doi.org/10.1016/0012-8252(93)90029-7.

Dawson, S. E., and Madsen, G. E., (2007). Uranium Mine Workers, Atomic Downwinders, and the Radiation Exposure Compensation Act. Half-Livesives & Half-Truths: Confronting the Radioactive Legacies of the Cold War, pp. 117–143. Santa Fe: School for Advanced Research.

DeSimone, L.A., McMahon, P.B., and Rosen, M.R., (2014). The quality of our Nation's waters—Water quality in Principal Aquifers of the United States, 1991–2010: U.S. Geological Survey Circular 1360, 151 p., *https://dx.doi.org/10.3133/cir1360*. ISSN 2330–5703.

De Roos, A. J., Ward, M. H., Lynch, C. F., & Cantor, K. P. (2003). Nitrate in public water supplies and the risk of colon and rectum cancers. *Epidemiology*, 640-649.

Drake, R.M., II, and Hatch, J.R., (2021). Geologic assessment of undiscovered oil and gas resources in the Cherokee Platform area of Kansas, Oklahoma, and Missouri: U.S. Geological Survey Scientific Investigations Report 2020–5110, 39 p.

Driscoll, C. T., Mason, R. P., Chan, H. M., Jacob, D. J., & Pirrone, N., (2013). Methylmercury in freshwater fish linked to atmospheric mercury deposition. Journal of Environmental Science & Technology. DOI: 10.1021/es3035682.

Duff, M., Hunter, D., Bertsch, P., Amrhein, C., (1999). Factors influencing uranium reduction and solubility in evaporation pond sediments. Biogeochemistry 45 (1), 95–114.

Dvorak, B. I., Skipton, S. O., Woldt, W. E., [2007], (2021). Drinking water; Iron and Manganese. G1714: Natural Resources / Water Management. https://extensionpublications.unl.edu/assets/html/g1714/build/g1714.html.

Environmental Protection Agency, (2000). National Primary Drinking Water Regulations; Radionuclides; Final Rule 40 CFR Vol. 65, No. 236 Parts 9, 141, and 142, Federal Register / / Thursday, Dec 7, Rules and Regulations.

Espejo-Herrera, N., Gràcia-Lavedan, E., Boldo, E., Aragonés, N., Pérez-Gómez, B., Pollán, M., & Villanueva, C. M. (2016). Colorectal cancer risk and nitrate exposure through drinking water and diet. *International journal of cancer*, *139*(2), 334-346.

Flewelling, S., Sharma, M., (2013). Constraints on Upward Migration of Hydraulic Fracturing Fluid and Brine. Groundwater. 52. 10.1111/gwat.12095. http://www.kgs.ku.edu/Publications/Bulletins/LA/03_gamma.html.

Freire, C., Ramos, R., Lopez-Espinosa, M. J., Díez, S., Vioque, J., Ballester, F., & Fernandez, M. F., (2010). Hair mercury levels, fish consumption, and cognitive development in preschool children from Granada, Spain. *Environmental research*, *110*(1), 96-104.

Fredrickson, J. K., Zachara, J. M., Kennedy, D. W., Liu, C., Duff, M. C., Hunter, D. B., Dohnalkova, A., (2002). Influence of Mn oxides on the reduction of uranium (VI) by the metal-reducing bacterium *Shewanella putrefaciens* Geochim. Cosmochim. Acta **2002**, 66 (18) 3247– 326229

Gilmour, C. C., Henry, E. A., & Mitchell, R., (1992). Microbial reduction of mercury and its impact on the biogeochemical cycle of mercury in the environment. Journal of Environmental Science & Technology. DOI: 10.1021/es00029a012.

Gosselin, R. E., Smith, R. P., Hodge, H. C., (1984). Clinical toxicology of commercial products, 5th ed. Baltimore, MD, Williams & Wilkins.

Hasan S. E., (2021). Medical Geology. Encyclopedia of Geology.:684–702. doi: 10.1016/B978-0-12-409548-9.12523-0. Epub 2020 Dec 2. PMCID: PMC7241403.

Hem, J. D., (1995). *Study and Interpretation of the Chemical Characteristics of Natural Water*; U.S. Geological Survey Water-Supply Paper: Washington, DC, USA; Volume 2254, p. 363.

Heyes, A., Miller, C. L., Mason, R. P., & Sunderland, E. M., (2006). Formation of methylmercury in a marine water column. Geochimica et Cosmochimica Acta. DOI: 10.1016/j.gca.2006.05.010.

Hu, H., Lin, H., Zheng, W. *et al.*, (2013). Oxidation and methylation of dissolved elemental mercury by anaerobic bacteria. *Nature Geosci* 6, 751–754 (2013). https://doi.org/10.1038/ngeo1894.

Huang, X., (2003). Iron overload and its association with cancer risk in humans: evidence for iron as a carcinogenic metal, Mutat. Res., 533 (2003), pp. 153-171.

Jennings, S. R., Blicker, P. S., & Neuman, D. R. (2008). *Acid mine drainage and effects on fish health and ecology: a review*. Reclamation Research Group.

Kansas Department of Health and Environment. Kansas Environmental Public Health Tracking Network. (n.d.) Web. Accessed: [30th December 2023] https://keap.kdhe.ks.gov/ephtm/.

Kansas Geological Survey (2013). Gamma Ray Sources in Rocks. Web accessed: [11th January 2024] http://www.kgs.ku.edu/Publications/Bulletins/LA/03_gamma.html.

Kansas Geological Survey, [1963], (2006) Geologic History of Kansas: URL = http://www.kgs.ku.edu/Publications/Bulletins/162/05_tect.html.

Kansas Historic Society [2003] (2022). Big Brutus, https://www.kshs.org/kansapedia/big-brutus/11981.

Kansas Historic Society [2016] (2018). Coal mining in southeast Kansas, https://www.kshs.org/kansapedia/coal-mining-in-southeast-kansas/19849.

Keith, S., Faroon, O., Roney, N., Scinicariello, F., Wilbur, S., Ingerman, L., Llados, F., Plewak, D., Wohlers, D., & Diamond, G., (2013). *Toxicological Profile for Uranium*. Agency for Toxic Substances and Disease Registry (US).

Kirk, Matthew F., "Microbiology for Earth Scientists" (2023). *NPP eBooks*. 53. https://newprairiepress.org/ebooks/53

King, J. K., Kostka, J. E., Frischer, M. E., & Saunders, F. M., (2000). Redox Transformations of Mercury in Anoxic Freshwater Sediments. Journal of Environmental Science & Technology. DOI:10.1021/es9912521.

Lapworth D. J., Brauns B., Chattopadhyay S, Gooddy D. C., Loveless S. E., MacDonald A. M., McKenzie A. A., Muddu S., Nara S. N. V., (2021). Elevated uranium in drinking water sources in basement aquifers of southern India, Applied Geochemistry, Volume 133, 105092, ISSN 0883-2927, https://doi.org/10.1016/j.apgeochem.2021.105092.

Lane, A.D., Kirk, M.F., Whittemore, D.O. *et al.* (2020). Long-term (the 1970s–2016) changes in groundwater geochemistry in the High Plains aquifer in south-central Kansas, USA. *Hydrogeol J* **28**, 491–501. https://doi.org/10.1007/s10040-019-02083-z.

Liu, C. X., Zachara, J. M., Fredrickson, J. K., Kennedy, D. W., Dohnalkova, A. (2002). Modeling the inhibition of the bacterial reduction of U(VI) by β-MnO_2(s) Environ. Sci. Technol. 2002, 36 (7) 1452– 1459

Lü X.L., Liu J. T., Han Z. T., Zhu L., Li H. J., (2022), Characteristics and Causes of High-manganese Groundwater in Pearl River Delta During Urbanization. Huan Jing Ke Xue.43(10):4449-4458. Chinese. doi: 10.13227/j.hjkx.202111136. PMID: 36224131.

Maslov, O. D.; Tserenpil, Sh.; Norov, N.; Gustova, M. V.; Filippov, M. F.; Belov, A. G.; Altangerel, M.; Enhbat, N., 2010. Uranium recovery from coal ash dumps of Mongolia. *Solid Fuel Chemistry*. **44** (6): 433–438. doi:10.3103/S0361521910060133.

McElroy, J. A., Trentham-Dietz, A., Gangnon, R. E., Hampton, J. M., Bersch, A. J., Kanarek, M. S., & Newcomb, P. A. (2008). Nitrogen-nitrate exposure from drinking water and colorectal cancer risk for rural women in Wisconsin, USA. *Journal of Water and Health*, *6*(3), 399-409.

Merriam D. F., (1963). The geologic history of Kansas: Kansas Geological Survey, Bulletin 162, 317 p.

Minnesota Department of Health, (2023). Iron in Well Water, Web Accessed [16th January 2024], https://www.health.state.mn.us/communities/environment/water/wells/waterquality/iron.html.

Minnesota Department of Health, (2023). Nitrate in Well Water. Web Accessed: [12th January 2024], https://www.health.state.mn.us/communities/environment/water/wells/waterquality/nitrate.html.

Morel, F. M. M., & Kraepiel, A. M. L., (1998). Formation of methylmercury in aquatic systems: An overview. Journal of Applied and Environmental Microbiology. DOI: 10.1128/AEM.64.12.4371-4378.1998.

Neidhardt, H., Berner, Z. A., Freikowski, D., Biswas, A., Majumder, S., Winter, J., & Norra, S. (2014). Organic carbon induced mobilization of iron and manganese in a West Bengal aquifer and the muted response of groundwater arsenic concentrations. *Chemical Geology*, *367*, 51-62.

Newell, K. D., Watney, W. L., Steeples, D. W., Knapp, R. W., (2013). Suitability of high-resolution seismic method to identifying petroleum reserves in Kansas – a geological perspective, Kansas Geological Survey Bulletin 226, pp. 9–29.

Nickson, R. T. Mcarthur, J. M., Ravenscroft, P., Burgess, W. G., Ahmed, K. M., (2000) Mechanism of arsenic release to groundwater, Bangladesh and West Bengal. *Appl. Geochem.* 2000, *15*, 403–413.

Niknahad, A. M., Ommati, M. M., Farshad, O., Moezi, L., Heidari, R., (2020). Manganese-Induced Nephrotoxicity Is Mediated through Oxidative Stress and Mitochondrial Impairment. *Journal of Renal and Hepatic Disorders*, *4*(2), 1-10. https://doi.org/10.15586/jrenhep.2020.66

Nolan, J., Weber, K., (2015). Natural Uranium Contamination in Major U.S. Aquifers Linked to Nitrate. *Environmental Science & Technology Letters* **2015** *2* (8), 215-220. DOI: 10.1021/acs.estlett.5b00174.

Nolan, P. J., Bone, S. E., Campbell, K. M., Pan, D., Healy, O. M., Stange, M., Bargar, J. R., Weber, K. A., (2021). Uranium (VI) attenuation in a carbonate-bearing oxic alluvial aquifer, Journal of Hazardous Materials, Volume 412, 125089, ISSN 0304-3894, https://doi.org/10.1016/j.jhazmat.2021.125089.

Ochieng, G, Seanego, E. & Nkwonta, O., (2010). Impacts of mining on water resources in South Africa: A review. Scientific Research and Essays. 5. 3351-3357.

O'Neil, J., & Powell, L. (2005, November). Clinical aspects of hemochromatosis. In *Seminars in liver disease* (Vol. 25, No. 04, pp. 381-391). Copyright© 2005 by Thieme Medical Publishers, Inc., 333 Seventh Avenue, New York, NY 10001, USA.

Ontheworldmap.com., (2024). Kansas Location on the U.S, Map. Web Accessed [11th February 2024]. https://ontheworldmap.com/usa/state/kansas/kansas-location-on-the-us-map.html.

Papanikolaou, G., & Pantopoulos, K. (2005). Iron metabolism and toxicity. *Toxicology and Applied Pharmacology*, *202*(2), 199-211. https://doi.org/10.1016/j.taap.2004.06.021.

Parviainen A., Loukola-Ruskeeniemi K., (2019). Environmental impact of mineralised black shales. Earth-Science Reviews, Volume 192, Pages 65-90, ISSN 0012-8252, https://doi.org/10.1016/j.earscirev.2019.01.017.

Post, J. E., (1999). Manganese oxide minerals: Crystal structures and economic and environmental significance, 1999, Proceedings of the National Academy of Sciences, p 3447-3454, 96, 7, doi:10.1073/pnas.96.7.3447, https://www.pnas.org/doi/abs/10.1073/pnas.96.7.3447

Prasad, M. N. V., Nakbanpote, W., Phadermrod, C., Rose, D., Suthari, S., (2016). Chapter 13 - Mulberry and Vetiver for Phytostabilization of Mine Overburden: Cogeneration of Economic Products, Editor(s): M.N.V. Prasad, Bioremediation and Bioeconomy,

Elsevier, Pages 295-328, ISBN 9780128028308, https://doi.org/10.1016/B978-0-12-802830-8.00013-7

Ramm, G. A., & Ruddell, R. G. (2005). Hepatotoxicity of iron overload: mechanisms of iron-induced hepatic fibrogenesis. In *Seminars in liver disease* (Vol. 25, No. 04, pp. 433-449). Copyright© 2005 by Thieme Medical Publishers, Inc., 333 Seventh Avenue, New York, NY 10001, USA.

Ranken, R. A., (1998). U.S. Geological Surve. Hydrologic Atlas; Groundwater Atlas of the United States. HA 730-F. Web Accessed [13th January 2023], https://pubs.usgs.gov/ha/ha730/ch_f/F-text6.html.

Ravalli, F., Yu Y., Bostick B. C., Chillrud S. N., Schilling k., Basu A, Navas-Acien A., Nigra A. E., (2022). Sociodemographic inequalities in uranium and other metals in community water systems across the USA, 2006-11: a cross-sectional study, Lancet Planet. Health, 6 , pp. e320-e330, 10.1016/S2542-5196(22)00043-2.

Ravichandran, M., (2004). Abiotic Reduction of Mercury by humic substance in aquatic systems. Journal of Environmental Science & Technology. DOI: 10.1071/EN09009.

Rice, K. M., Walker, E. M., Wu, M., Gillette, C., Blough, E. R., (2014) Environmental Mercury and Its Toxic Effects. J Prev Med Public Health. 2014;47(2):74-83.

Riley, R. G.; Zachara, J. M.; Wobber, F. J., (1992). "Chemical contaminants on DOE lands and selection of contaminant mixtures for subsurface science research," U.S. Department of Energy.

Rudi, N. N., Muhamad, M. S., Chuan, L. T., Alipal, J., Omar, S., Hamidon, N., Abdul Hamid, N., Sunar, N. M., Ali, R., Harun, H., (2020). Evolution of adsorption process for manganese removal in water via agricultural waste adsorbents, Heliyon, Volume 6, Issue 9, e05049, ISSN 2405-8440, https://doi.org/10.1016/j.heliyon.2020.e05049. (https://www.sciencedirect.com/science/article/pii/S2405844020318922).

Saha, S., Reza, A.H.M.S. & Roy, M.K., (2019). Hydrochemical evaluation of groundwater quality of the Tista floodplain, Rangpur, Bangladesh. *Appl Water Sci* **9**, 198 (2019). https://doi-org.er.lib.k-state.edu/10.1007/s13201-019-1085-7

Schullehner, J., Hansen, B., Thygesen, M., Pedersen, C. B., & Sigsgaard, T. (2018). Nitrate in drinking water and colorectal cancer risk: A nationwide population-based cohort study. *International journal of cancer*, *143*(1), 73–79. https://doi.org/10.1002/ijc.31306.

Stewart B. D., Melanie A. M., Scott F., (2010). Impact of Uranyl-Calcium-Carbonate Complexes on Uranium (VI) Adsorption to Synthetic and Natural Sediments. *Environmental Science & Technology 44* (3), 928-934 DOI: 10.1021/es902194x.

Tchounwou, P. B., Yedjou, C. G., Patlolla, A. K., Sutton, D. J., (2012). Heavy metal toxicity and the environment. Exp Suppl. 2012;101:133-64. doi: 10.1007/978-3-7643-8340-4_6. PMID: 22945569; PMCID: PMC4144270.

Tedesco, S. A., (2014), Reservoir characterization and geology of the coals and carbonaceous shales of the Cherokee Group in the Cherokee Basin, Kansas, Missouri and Oklahoma, U.S.A: ProQuest Dissertations Publishing.

Tirmarche M., Baysson H., Telle-Lamberton M., (2004). Uranium exposure and cancer risk: a review of epidemiological studies]. Rev Epidemiol. Sante Publique. Feb;52(1): p.81-90. French. doi: 10.1016/s0398-7620(04)99024-4. PMID: 15107695.

U.S. Department of Health & Human Service, Center for Disease Control and Prevention, (2022). Disinfection By-products (DBPs), Web Accessed [16th January 2024], https://www.cdc.gov/biomonitoring/THM-DBP_FactSheet.html#:~:text=Chronic%20exposure%20to%20DBPs%20may,and%20decreased%20nervous%20system%20activity.

U.S. Department of Health & Human Service, National Cancer Institute. State Cancer Profiles, Web Accessed [16th January 2024], https://statecancerprofiles.cancer.gov/help/about/incidence_rates.

U.S. Department of Health and Human Services. (1995). PHS. *ATSDR Toxicological Profile for Polycyclic Aromatic Hydrocarbons (PAHs), Atlanta, GA.*

U.S. Environmental Protection Agency, (2021). Community Guide to Granular Activated Carbon Treatment. Office of Land and Emergency Management (5203P), EPA-542-F-21-010.

U.S. Environmental Protection Agency, (2021). Addressing Manganese in Drinking Water with the Drinking Water State Revolving Fund. EPA 816-F-21-001, Web Accessed [15th January 2024], chrome-extension://efaidnbmnnnibpcajpcglclefindmkaj/https://www.epa.gov/system/files/documents/2021-09/addressing-manganese-with-the-dwsrf-and-case-studies_final_2.pdf.

U.S. Environmental Protection Agency, (2021). Addressing Nitrate with the DWSRF. EPA 816-F-20-005, Web Accessed [15th January 2024], chrome-extension://efaidnbmnnnibpcajpcglclefindmkaj/https://www.epa.gov/sites/default/files/2021-06/documents/addressing_nitrates_with_the_dwsrf-final.pdf.

U.S. Environmental Protection Agency. Health Effects Support Document for Manganese. [(accessed on 30 January 2009)]. Available online: http://www.epa.gov/safewater/ccl/pdf/manganese.pdf.

U.S. Environmental Protection Agency, (2024). National Primary Drinking Water Regulations. Web Accessed [14th January, 2024], https://www.epa.gov/ground-water-and-drinking-water/national-primary-drinking-water-regulations.

U.S. Environmental Protection Agency, (2002). Nitrification. Web accessed: 12th January 2024. https://www.epa.gov/sites/default/files/2015-09/documents/nitrification_1.pdf.

U.S. Geological Survey. (2019). Mercury. Web accessed; [14th January 2024], https://www.usgs.gov/mission-areas/water-resources/science/mercury.

Velasco, C. A., Brearley, A. J., Gonzalez-Estrella, J., Ali, A. S., Meza, M., I., Cabaniss, S. E., Thomson, B. M., Forbes, T. Z., Lezama Pacheco, J. S., Cerrato, J.M., (2021). From Adsorption to Precipitation of U(VI): What is the Role of pH and Natural Organic Matter? Environ Sci Technol. 2021 Dec 7;55(23):16246-16256. doi: 10.1021/acs.est.1c05429. Epub 2021 Nov 19. PMID: 34797046; PMCID: PMC8680647.

Wang, Z., Lee S., Catalano J. G., Lezama-Pacheco J. S., Bargar J. R., Tebo B. M., and Giammar D. E., (2013). Adsorption of Uranium (VI) to manganese Oxides: Xray Adsorption Spectroscopy and Surface Complexation Modelling. *Environmental Science & Technology* **2013** *47* (2), 850-858, DOI: 10.1021/es304454g

Washington State Department of Health, (2022). Nitrate in Drinking Water. Fact Sheet. 331-214. chrome-extension://efaidnbmnnnibpcajpcglclefindmkaj/https://doh.wa.gov/sites/default/files/legacy/Documents/Pubs/331-214.pdf.

Ward, M. H., Jones, R. R., Brender, J. D., De Kok, T. M., Weyer, P. J., Nolan, B. T., Villanueva, C. M., & Van Breda, S. G. (2018). Drinking Water Nitrate and Human Health: An Updated Review. *International Journal of Environmental Research and Public Health*, *15*(7), 1557. https://doi.org/10.3390/ijerph15071557.

Wentz, D. A., Brigham, M. E., Chasar, L. C., Lutz, M. A., and Krabbenhoft, D. P., (2014), Mercury in the Nation's streams—Levels, trends, and implications: U.S. Geological Survey Circular 1395, 90 p., https://dx.doi.org/10.3133/cir1395. ISSN 2330-5703

West, R. R., and Sawin, R. S., and Bradly, L. L., (2000). Surficial Geology of Crawford County, Kansas: Kansas Geological Survey, Map M-120, scale 1:50,000.

West, R. R., and Saw in, R. S., [2002] (2020). Surficial Geology of Bourbon County, Kansas: Kansas Geological Survey, Map M-97 (revised), scale 1:50,000.

World Health Organization, (2009). Potassium in Drinking-Water Web Accessed [15th January 2009]. Available online: chrome-extension://efaidnbmnnnibpcajpcglclefindmkaj/https://cdn.who.int/media/docs/default-source/wash-documents/wash-chemicals/potassium-background.pdf?sfvrsn=4542eda3_4.

World Health Organization, (2017). Guidelines for Drinking-Water Quality, 4th Edition, Incorporating the 1st Addendum, ISBN: 978-92-4-154885-0.

Zhang, Z., Xiao, C., Adeyeye, O., Yang, W., Liang, X., (2020) Source and Mobilization Mechanism of Iron, Manganese and Arsenic in Groundwater of Shuangliao City, Northeast China. *Water*. 12(2):534.

Appendix A - Additional Information

Table A.1: Gamma ray data.

S/N	Well KID	API No.	Latitude	Longitude	Cumulative Thick. 150 API (ft)	County
1	1031639174	15-011-23011	37.891455	-94.812883	3.73	Bourbon
2	1002887259	15-011-20283	37.877732	-94.66923	0	Bourbon
3	1002887260	15-011-20284	37.836186	-94.631106	2.3	Bourbon
4	1031891833	15-011-22746	37.931064	-95.066388	12.22	Bourbon
5	1006343809	15-011-22766	38.021412	-95.073028	35	Bourbon
6	1030624876	15-011-20431	37.936439	-95.056756	11.98	Bourbon
7	1030625051	15-011-22675	37.763864	-95.073932	43.49	Bourbon
8	1033438560	15-011-23133	37.697404	-94.986754	14.5	Bourbon
9	1025687182	15-011-22923	37.835164	-95.060021	8.81	Bourbon
10	1002887261	15-011-20285	37.746957	-94.777427	0	Bourbon
11	1002887264	15-011-20288	37.687897	-94.629981	37.4	Bourbon
12	1002887273	15-011-20302	37.703761	-94.917865	0	Bourbon
13	1031002320	15-011-22982	37.959427	-94.75225	57.3	Bourbon
14	1031639174	15-011-23011	37.891455	-94.812883	10.6	Bourbon
15	1025687181	15-011-22922	37.759962	-94.975306	16.25	Bourbon
16	1002887856	15-011-22850	37.817706	-95.053622	0.4	Bourbon
17	1044119799	15-011-23996	37.90395	-94.82888	86.55	Bourbon
18	1033438572	15-011-23139	37.692758	-94.989157	11.4	Bourbon
19	1036762235	15-011-23250	38.02553	-94.914117	10.8	Bourbon
20	1031996735	15-011-23081	37.744986	-94.931337	60.8	Bourbon
21	1031891887	15-011-23032	37.995425	-94.790195	21.21	Bourbon
22	1040860117	15-011-23626	38.002798	-94.962516	13	Bourbon
23	1025687182	15-011-22923	37.835164	-95.060021	10.89	Bourbon
24	1044760457	15-011-24408	37.855459	-95.01722	24.61	Bourbon
25	1044754238	15-011-24403	37.852077	-95.011394	52.15	Bourbon
26	1029098241	15-011-21953	37.776807	-94.885764	18.3	Bourbon
27	1044653783	15-011-24395	37.8559	-95.020426	25.53	Bourbon
28	1044653783	15-011-24393	37.8559	-95.020426	96.54	Bourbon
29	1044653782	15-011-24394	37.861437	-95.022446	13.82	Bourbon
30	1003527702	15-011-22091	37.779586	-94.875541	12	Bourbon
31	1043122366	15-011-23771	37.899031	-94.816725	121	Bourbon
32	1043122329	15-011-23775	37.999184	-94.66553	105	Bourbon
33	1044661393	15-011-24397	37.878264	-95.042227	102.21	Bourbon
34	1043122382	15-011-23774	37.999194	-94.666675	108	Bourbon
35	1044666092	15-011-24398	37.859516	-95.017953	40.34	Bourbon
36	1044653781	15-011-24393	37.860111	-95.012875	37.55	Bourbon

37	1044634484	15-011-24376	38.009235	-95.043144	13.4	Bourbon
38	1036443797	15-011-23238	37.730594	-94.843072	3.9	Bourbon
39	1031996727	15-011-23077	37.745355	-94.834194	146	Bourbon
40	1043560823	15-011-23801	37.68774	-94.626319	0	Bourbon
41	1020066502	15-011-22917	37.773559	-94.649671	175.25	Bourbon
42	1002887582	15-011-21945	37.780459	-94.881266	16	Bourbon
43	1002887261	15-011-20285	37.746957	-94.777427	0	Bourbon
44	1031522981	15-011-22999	37.70276	-94.971041	0	Bourbon
45	1030625114	15-011-22399	37.678943	-95.047675	10.5	Bourbon
46	1031535318	15-011-23008	37.770742	-94.889191	6	Bourbon
47	1030570908	15-011-22968	37.719826	-94.888879	14	Bourbon
48	1030615776	15-037-20401	37.425807	-95.071773	39.2	Crawford
49	1002906235	15-037-20451	37.39604	-95.08714	35.6	Crawford
50	1002906207	15-037-20348	37.408893	-95.080956	31.4	Crawford
51	1002906208	15-037-20349	37.429459	-95.080785	34.7	Crawford
52	1025824935	15-037-21257	37.669009	-95.041444	22.5	Crawford
53	1025824841	15-037-21197	37.58602	-94.997103	25.6	Crawford
54	1002906372	15-037-21476	37.564205	-95.007602	21.4	Crawford
55	1005423248	West Well WS	37.343808	-94.828537	17.5	Crawford
56	1030614603	15-037-21622	37.600313	-94.845172	11.4	Crawford
57	1030614603	15-037-21622	37.600313	-94.845172	37.8	Crawford
58	1031938397	15-037-21663	37.614139	-95.052636	18.2	Crawford
59	1036126013	15-037-21862	37.419176	-95.040266	13.8	Crawford
60	1042911665	15-037-22120	37.43787	-95.042871	20.2	Crawford
61	1032690803	15-037-21721	37.673402	-94.867944	1.5	Crawford
62	1035940771	15-037-21836	37.343061	-95.063391	7.6	Crawford
63	1031431059	15-037-21656	37.622188	-95.086229	9.7	Crawford
64	1031996857	15-037-21677	37.650473	-94.867273	17.4	Crawford
65	1038329980	15-037-22059	37.542488	-94.895219	31.5	Crawford
66	1041343762	15-037-22094	37.396128	-95.026943	19	Crawford
67	1030570986	15-037-21603	37.660833	-94.858462	30.9	Crawford
68	1030570996	15-037-21608	37.54196	-94.834424	23.3	Crawford
69	1025824659	15-037-22061	37.548351	-94.868345	40.5	Crawford
70	1042911665	15-037-22120	37.43787	-95.042871	32	Crawford
71	1038465368	15-037-22069	37.616116	-94.693914	22.1	Crawford
72	1030570998	15-037-21609	37.556849	-94.873393	31.8	Crawford
73	1042911625	15-037-22125	37.436958	-95.041736	24.8	Crawford
74	1044888225	15-037-22289	37.373888	-95.048535	29	Crawford
75	1046466515	15-037-22344	37.380553	-95.052173	18.8	Crawford
76	1046492412	15-037-22362	37.56742	-95.064086	22.1	Crawford
77	1043460492	15-037-22167	37.426913	-95.046868	3.57	Crawford
78	1002906178	15-037-20238	37.658676	-94.647893	0	Crawford
79	1002906179	15-037-20240	37.614006	-94.777452	0.39	Crawford
80	1002906180	15-037-20241	37.572183	-94.670794	0	Crawford
81	1002906181	15-037-20242	37.557097	-94.778575	5.18	Crawford

82	1002906182	15-037-20244	37.484274	-94.771969	0.3	Crawford
83	1002906184	15-037-20247	37.39672	-94.788181	0	Crawford
84	1002906185	15-037-20248	37.451505	-94.649212	0	Crawford
85	1002906190	15-037-20253	37.471032	-94.905563	0	Crawford
86	1002906191	15-037-20254	37.498666	-94.651126	0.14	Crawford
87	1043460489	15-037-22164	37.42418	-95.044031	10.21	Crawford
88	1046466478	15-037-22348	37.380001	-95.049263	17.97	Crawford

Table A.2: Field Data.

	Lat	Long	Elevation	Depth-to-Water	Total Depth	pH	Temp.	Cond.	DO	Spec. Cond.
Bo-1b	37.76	-94.88	297.64	3.32	5.79	7.05	16.7	1214	1.81	1286
Bo-3	38.03	-94.69	260.66	2.09	5.12	7.18	16.3	721	9.26	670
Bo-4a	37.83	-95.02	307.43	3.69	6.98	7.08	15.3	654.4	1.8	660
Bo-4b	37.84	-95.04	325.61	3.41	6.19	7.51	16.9	1217	3.81	1205
Bo-5	37.83	-95.06	337.33	4.33	20.42	7.51	13.5	613	1.01	0.8
Bo-6a	37.81	-95.06	291.11	0.64	1.10	7.51	19.5	662.5	3.9	331.6
Bo-6b	37.83	-95.1	324	2.41	6.14	7.04	14.5	679.4	2.34	707
Bo-6c	37.83	-95.1	306	0.00	0.00	6.73	24.8	506.2	3.58	298.5
Bo-6d	37.83	-95.1	312.71	4.33	33.77	6.9	14	673	1.55	367
Bo-6e	37.84	-95.1	325.57	5.88	14.29	6.98	14.2	1018	1.7	4
Bo-6f	37.85	-95.11	324	2.93	4.36	6.87	14	405	1.07	3
Bo-7a	37.9	-94.88	280.36	2.74	5.94	7.48	14	676.6	1.63	397.2
Bo-7b	37.9	-94.88	276.85	2.04	6.55	7.46	14.9	470.2	1.6	109.2
Bo-7c	37.9	-95.07	280.36	2.04	9.63	7.46	16.2	319.6	4.58	168.2
Bo-8	38.007	-94.72	260.03	1.89	5.88	7.33	13.8	308.7	1.64	156.2
Bo-9	37.743	-95.07	333.12	1.25	4.15	7.05	16	446.1	2.7	9.3
Cr-1b	37.54	-94.62	284.09	73.15	169.16	7.35	21.2	1595	3.44	8.7
Cr-2	37.58	-94.81	303.75	2.80	10.36	7.96	16.4	665.1	1.25	346.7
Cr-3	37.53	-94.67	297.04	1.07	1.58	6.99	19	544.3	2.11	7.4
Cr-4	37.53	-94.68	301.99	2.38	8.69	7.2	15.9	1058	6.53	4.1
Cr-5	37.6	-94.65	270.93	1.68	3.47	6.91	15.7	477.2	1.77	344.4
Cr-6	37.46	-94.68	297.58	111.25	307.83	7.11	21.3	1310	2.46	1349
Cr-7	37.403	-94.67	282.92	106.67	350.50	7.1	20.6	1016	4.7	954
Ch-1	37.12	-94.84	281.45	60.96	154.53	6.94	19.5	1102	5	992
Ch-2	37.58	-94.81	270.95	30.48	63.09	6.93	23.1	1100	5.6	1000
Ch-3	37.1	-94.63	282.69			7.02	19.5	346.3	0.7	305.8
Ch-4	37.63	-94.63	306.38		60.96	6.85	17	425.9	3.73	365.1
Ch-5	37.03	-94.64	306.28		91.44	7.88	16.6	321.4	3.79	288
Ch-6	37.02	-94.63	307.56		121.91	6.99	17.94	410.8	5.65	369.1
Ch-7	37.02	-94.63	303.97		91.44	6.76	17.1	386.9	6.7	343.9
Ch-8	37.031	-94.67	281.6		35.96	6.85	16.5	420.9	6.01	370
Ch-9	37.033	-94.67	290.05		30.48	6.92	16.7	409	5	344.2
Ch-10	37.02	-94.69	278.7		121.91	6.96	17.6	368.6	7	325.8
Ch-11	37.024	-94.62	316.02		42.67	7.28	17.1	300.4	4.35	278
Ch-12	37.02	-94.70	272.9	18.29	54.86	7.29	16.8	309.8	8.12	285.1
Ch-13	37.01	-95	252.33		68.58	6.27	17.6	982.9	1.5	925
Ch-14	37.33	-95.01	268.16	2.16	7.35	7.17	15.4	798.9	1.6	782
Ch-15a	37.28	-94.68	263.64	3.35	4.66	6.55	15.6	1433	6.7	133.9
Ch-15b	37.28	-94.68	266.47	3.32	6.19	6.85	15	679.8	4.8	665
Ch-15c	37.28	-94.68	263.1		77.72	6.72	17.9	840	4.6	826

Ch-16	37.28	-94.91	270.18	2.29	3.20	7.07	17.6	473.6	1.68	449
Ch-17	37.16	-95.03	251.61	2.36	5.61	6.95	16.6	1200	1.81	2009
Ch-18	37.02	-95	244.8			7.67	18.7	1078	1.32	979

Table A.3: Anions concentrations in water samples.

	Chloride (mg/L)	Nitrite as N (mg/L)	Bromide (mg/L)	Nitrate as N (mg/L)	Phosphate (mg/L)	Sulfate (mg/L)
B0-1b	200.3	0	0.35	21.85	0.36	104.70
B0-3	29.44	0.04	0.03	8.17	6.44	68.60
B0-4a	16.52	0.00	0.04	13.16	2.47	25.16
B0-4b	87.9	0.00	0.49	0.02	8.17	97.80
B0-5	17.35	0.05	0.13	2.82	2.44	61.82
B0-6a	32.75	0.08	0.08	1.94	4.54	45.36
B0-6b	29.7	0.14	0.04	21.27	2.55	78.53
B0-6c	5.95	0	0.03	0.05	1.33	21.64
B0-6d	17.53	0	0.05	0	0.35	16.57
B0-6e	8.87	0.06	0.00	0.01	0.28	2.36
B0-6f	2.196	0.06	0.03	0.70	0.38	10.58
B0-7a	57.94	0.00	0.16	1.18	6.57	65.75
B0-7b	13.93	0.00	0.07	0.03	3.65	42.89
B0-7c	10.95	0.00	0.07	3.40	2.90	15.15
B0-8	5.974	0.09	0.03	0.39	3.12	16.52
B0-9	3.957	0.00	0.00	1.81	0.66	13.75
Cr-1b	60.46	0.00	0.00	0.06	0.41	0.36
Cr-2	12.63	0.00	0.08	0.03	1.27	0.02
Cr-3	20.39	0.00	0.05	0.06	5.92	99.07
Cr-4	78.73	0.00	0.38	2.93	0.82	239.60
Cr-5	9.365	0.06	0.07	0.45	1.31	106.50
Cr-6	266.6	0	0.70	0.00	0.00	39.44
Cr-7	129.7	0	0.34	0.02	6.35	50.40
Cr-1	61.7	0	0.17	0.00	1.61	233.90
Cr-2	5.382	0	0.03	0.03	0.50	320.60
Cr-3	1.524	0	0.02	0.00	0.34	19.93
Cr-4	4.331	0	0.04	0.77	0.80	6.73
Cr-5	2.784	0	0.02	0.00	0.21	4.42
Cr-6	2.094	0	0.02	0.18	0.23	5.94
Cr-7	5.489	0	0.04	1.80	0.29	10.60
Cr-8	3.102	0	0.06	0.92	0.00	7.54
Cr-9	2.798	0	0.05	0.51	0.14	8.71
Cr-10	1.471	0	0.05	0.32	0.01	9.59
Cr-11	2.887	0	0.04	0.08	0.28	16.57
Cr-12	2.312	0	0.05	1.75	0.17	9.59
Cr-13	16.91	0	0.00	4.73	0.03	372.70
Cr-14	42.96	0	0.16	1.34	0.00	153.00
Cr-15a	3.3	0	0.00	0.49	1.03	27.62
Cr-15b	70.12	0	0.16	3.92	1.73	102.00
Cr-15c	11.9	0	0.05	0.03	0.05	197.50
Cr-16	25.04	0	0.12	0.26	6.34	37.76

Cr-17	300	0	1.05	16.73	1.30	249.90
Cr-18	103	0	0.38	0.00	0.00	68.19

Table A.4: Cation concentrations in water samples.

	Sodium (mg/L)	Ammonium (mg/L)	Potassium (mg/L)	Magnesium (mg/L)	Calcium (mg/L)	Strontium (mg/L)
Bo-1b	40.39	0.00	3.48	60.67	145.10	6.17
Bo-3	21.82	0.00	13.20	15.11	87.25	2.86
Bo-4a	9.28	0.00	8.12	4.47	122.10	3.17
Bo-4b	44.01	0.00	44.80	18.79	171.50	0.00
Bo-5	23.44	0.00	11.00	10.54	99.56	3.13
Bo-6a	14.76	0.00	19.97	11.79	110.00	3.15
Bo-6b	41.91	1.36	6.73	5.92	98.77	2.64
Bo-6c	3.19	0.00	3.07	3.81	114.90	2.58
Bo-6d	5.21	1.59	15.15	5.55	136.10	2.96
Bo-6e	5.60	8.35	14.24	5.42	140.90	3.16
Bo-6f	3.81	0.01	0.82	4.13	86.85	2.30
Bo-7a	31.69	0.00	34.46	14.74	88.65	2.79
Bo-7b	17.51	0.00	16.01	17.33	65.26	2.51
Bo-7c	20.63	0.00	5.32	6.09	38.47	1.40
Bo-8	5.18	0.00	18.72	5.95	44.28	1.29
Bo-9	3.28	0.00	1.12	4.57	91.36	2.47
Cr-1b	415.60	6.53	8.84	8.81	15.55	1.97
Cr-2	164.10	3.40	4.55	6.58	9.21	2.25
Cr-3	9.52	0.20	14.24	6.96	113.40	2.22
Cr-4	102.70	0.76	14.45	28.84	93.61	3.07
Cr-5	26.55	2.63	9.87	11.27	49.03	1.48
Cr-6	161.10	1.86	6.47	32.48	71.19	3.33
Cr-7	109.50	0.80	16.50	27.60	61.55	2.84
Ch-1	81.03	0.27	11.29	28.74	107.20	3.43
Ch-2	23.59	0.00	3.29	29.33	163.40	4.97
Ch-3	5.90	0.00	0.52	3.02	61.15	0.00
Ch-4	4.98	0.00	1.24	1.69	72.75	0.00
Ch-5	4.59	0.00	0.33	1.65	78.05	1.48
Ch-6	5.86	0.00	1.88	14.46	38.83	0.00
Ch-7	6.11	0.00	0.83	1.24	67.44	0.00
Ch-8	2.15	0.04	0.34	1.95	80.38	0.00
Ch-9	2.33	0.05	0.61	2.97	76.28	1.36
Ch-10	1.76	0.05	0.48	1.31	71.40	0.00
Ch-11	3.82	0.07	1.76	14.34	36.09	0.91
Ch-12	1.77	0.04	0.39	2.33	56.11	0.00
Ch-13	91.76	0.00	1.17	24.66	68.85	2.12
Ch-14	36.39	0.52	1.80	18.04	111.40	3.02
Ch-15a	5.20	0.28	3.17	2.63	15.01	0.64
Ch-15b	63.06	0.66	3.30	14.45	55.55	1.49
Ch-15c	25.02	0.78	2.74	20.96	131.50	3.27
Ch-16	24.37	0.00	13.68	7.42	53.92	1.99

Ch-17	152.20	0.00	7.33	27.45	231.90	6.52
Ch-18	191.60	2.69	5.43	10.92	26.32	1.55

Table A.5: Trace metals concentrations in water samples in mg/L (ppm). Values were rounded-up to two decimal places.

	Li	B	S	Mn	Fe	Cu	Zn	Hg	Pb	U	Ni	Co	As	Se	Mo	Cd
Bo-1b	0.10	0.01	11.50	0.00	0.01	0.00	0.00	0.00	0.00	0.01	0.00	0.00	0.00	0.00	0.00	0.00
Bo-3	0.09	0.00	5.87	0.00	0.00	0.00	0.00	0.00	0.00	0.01	0.00	0.00	0.00	0.00	0.00	0.00
Bo-4a	0.09	0.00	1.63	0.01	0.00	0.00	0.00	0.00	0.00	0.01	0.00	0.00	0.00	0.00	0.00	0.00
Bo-4b	0.06	0.00	14.00	0.48	0.02	0.01	0.00	0.01	0.01	0.01	0.00	0.00	0.00	0.00	0.00	0.00
Bo-5	0.09	0.00	6.50	0.01	0.00	0.00	0.00	0.00	0.00	0.01	0.00	0.00	0.00	0.00	0.00	0.00
Bo-6a	0.09	0.00	4.83	0.25	0.03	0.00	0.00	0.00	0.00	0.02	0.00	0.00	0.00	0.00	0.00	0.00
Bo-6b	0.08	0.00	9.57	0.02	0.00	0.00	0.04	0.00	0.00	0.02	0.00	0.00	0.00	0.00	0.00	0.00
Bo-6c	0.07	0.00	1.90	0.14	0.05	0.00	0.00	0.00	0.00	0.01	0.00	0.00	0.00	0.00	0.00	0.00
Bo-6d	0.07	0.00	0.00	0.18	11.17	0.00	0.04	0.00	0.00	0.00	0.00	0.00	0.00	0.00	0.00	0.00
Bo-6e	0.08	0.00	1.27	0.26	2.57	0.00	0.00	0.00	0.00	0.01	0.00	0.00	0.00	0.00	0.00	0.00
Bo-6f	0.07	0.00	0.60	0.41	0.10	0.00	0.00	0.00	0.00	0.01	0.00	0.00	0.00	0.00	0.00	0.00
Bo-7a	0.07	0.00	7.30	0.01	0.03	0.00	0.00	0.00	0.00	0.02	0.00	0.00	0.00	0.00	0.00	0.00
Bo-7b	0.07	0.00	5.73	0.22	0.04	0.00	0.00	0.00	0.00	0.01	0.00	0.00	0.00	0.00	0.00	0.00
Bo-7c	0.06	0.00	1.30	0.00	0.00	0.00	0.00	0.00	0.00	0.01	0.00	0.00	0.00	0.00	0.00	0.00
Bo-8	0.06	0.00	1.37	0.06	0.01	0.00	0.00	0.00	0.00	0.00	0.00	0.00	0.00	0.00	0.00	0.00
Bo-9	0.06	0.00	1.43	0.01	0.00	0.00	0.00	0.00	0.00	0.01	0.00	0.00	0.00	0.00	0.00	0.00
Cr-1b	0.16	0.24	0.00	0.00	0.01	0.00	0.00	0.00	0.00	0.00	0.00	0.00	0.00	0.00	0.00	0.00
Cr-2	0.08	0.37	0.00	0.01	0.07	0.00	0.00	0.00	0.00	0.00	0.00	0.00	0.00	0.00	0.00	0.00
Cr-3	0.06	0.01	15.17	1.14	0.12	0.00	0.00	0.00	0.00	0.00	0.00	0.00	0.00	0.00	0.00	0.00
Cr-4	0.02	0.09	68.77	0.02	0.01	0.01	0.01	0.00	0.00	0.01	0.00	0.00	0.00	0.01	0.00	0.00
Cr-5	0.00	0.04	39.47	3.30	1.21	0.00	0.01	0.00	0.00	0.00	0.00	0.00	0.00	0.00	0.00	0.00
Cr-6	0.12	0.20	13.97	0.00	0.02	0.05	0.00	0.01	0.00	0.00	0.00	0.00	0.00	0.00	0.00	0.00
Cr-7	0.09	0.19	16.40	0.00	0.01	0.00	0.00	0.00	0.00	0.00	0.00	0.00	0.00	0.00	0.00	0.00
Ch-1	0.08	0.17	85.90	0.29	3.15	0.00	0.00	0.00	0.00	0.00	0.00	0.00	0.00	0.00	0.00	0.00
Ch-2	0.05	0.11	129.60	0.19	0.60	0.01	0.05	0.00	0.00	0.01	0.00	0.00	0.00	0.00	0.00	0.00
Ch-3	0.00	0.02	5.80	0.05	0.12	0.00	0.03	0.00	0.00	0.00	0.01	0.00	0.00	0.00	0.00	0.00
Ch-4	0.00	0.02	1.83	0.00	0.01	0.00	0.00	0.00	0.00	0.01	0.00	0.00	0.00	0.00	0.00	0.00
Ch-5	0.01	0.04	1.20	0.00	0.01	0.00	0.00	0.00	0.00	0.00	0.00	0.00	0.00	0.00	0.00	0.00
Ch-6	0.00	0.02	0.77	0.00	0.00	0.00	0.00	0.00	0.00	0.01	0.00	0.00	0.00	0.00	0.00	0.00
Ch-7	0.00	0.02	4.17	0.01	0.02	0.02	0.02	0.01	0.01	0.00	0.00	0.00	0.00	0.00	0.00	0.00
Ch-8	0.00	0.01	1.60	0.00	0.00	0.00	0.04	0.00	0.00	0.00	0.00	0.00	0.00	0.00	0.00	0.00
Ch-9	0.00	0.01	2.03	0.00	0.01	0.01	0.00	0.00	0.00	0.01	0.00	0.00	0.00	0.00	0.00	0.00
Ch-10	0.00	0.01	2.60	0.00	0.03	0.01	0.01	0.00	0.00	0.00	0.00	0.00	0.00	0.01	0.00	0.00
Ch-11	0.01	0.05	4.23	0.00	0.05	0.00	0.45	0.00	0.00	0.00	0.00	0.00	0.00	0.00	0.00	0.00
Ch-12	0.00	0.02	2.50	0.00	0.00	0.00	0.00	0.00	0.00	0.01	0.00	0.00	0.00	0.00	0.00	0.00
Ch-13	0.07	0.03	128.67	0.08	0.03	0.02	0.00	0.00	0.00	0.00	0.00	0.00	0.00	0.00	0.00	0.00
Ch-14	0.00	0.09	50.90	0.55	0.08	0.00	0.00	0.00	0.00	0.04	0.00	0.00	0.00	0.01	0.00	0.00
Ch-15a	0.00	0.03	8.40	0.01	0.01	0.00	0.01	0.00	0.00	0.00	0.00	0.00	0.00	0.00	0.00	0.00
Ch-15b	0.01	0.07	39.27	0.00	0.02	0.00	0.00	0.00	0.00	0.00	0.00	0.00	0.00	0.00	0.00	0.00
Ch-15c	0.10	0.09	92.17	0.49	4.44	0.00	0.02	0.00	0.00	0.00	0.00	0.00	0.00	0.00	0.00	0.00
Ch-16	0.01	0.07	12.03	0.32	0.17	0.01	0.04	0.02	0.00	0.01	0.00	0.00	0.00	0.00	0.00	0.00

Ch-17	0.01	0.02	107.53	0.06	0.04	0.01	0.00	0.01	0.00	0.03	0.00	0.00	0.00	0.00	0.00	0.00
Ch-18	0.16	0.67	26.70	0.00	0.03	0.01	0.01	0.01	0.00	0.00	0.00	0.00	0.00	0.00	0.00	0.00

Table A.6: Geochemical modeling results.

	Water type	Charge imbalance (%)	Charge imbalance error (%)	Dissolved solids	Log O_2 activity	TDS (molal)	Eh
Bo-1b	Ca-Cl	0.01973	-1.473%	60.67	-4.243	1001	0.7921
Bo-3	Ca-HCO_3	0.00986	-3.467%	15.11	-3.536	581.7	0.7948
Bo-4a	Ca-HCO_3	0.01022	-3.62%	4.47	-4.247	631.4	0.7902
Bo-4b	Ca-HCO_3	0.01755	-1.193%	18.79	-3.921	870.9	0.7696
Bo-5	Ca-HCO_3	0.00999	-1.526%	10.54	-4.498	577.5	0.7611
Bo-6a	Ca-HCO_3	0.0107	-2.152%	11.79	-3.911	622.4	0.7698
Bo-6b	Ca-HCO_3	0.01038	-3.649%	5.92	-4.133	630.4	0.7943
Bo-6c	Ca-HCO_3	0.008971	0.5796%	3.81	-3.948	589.3	0.8154
Bo-6d	Ca-HCO_3	0.01117	-2.064%	5.55	-4.312	726.5	0.7999
Bo-6e	Ca-HCO_3	0.01259	-16.26%	5.42	-4.271	933.8	0.7958
Bo-6f	Ca-HCO_3	0.007102	-1.909%	4.13	-4.473	457.4	0.7993
Bo-7a	Ca-HCO_3	0.01069	-0.8843%	14.74	-4.29	614.7	0.7659
Bo-7b	Ca-HCO_3	0.008244	-2.001%	17.33	-4.298	480.9	0.767
Bo-7c	Ca-HCO_3	0.004756	-2.189%	6.09	-3.842	291.6	0.7737
Bo-8	Ca-HCO_3	0.004856	-2.892%	5.95	-4.288	299.4	0.7748
Bo-9	Ca-HCO_3	0.007464	-1.787%	4.57	-4.071	457	0.7946
Cr-1b	Na-HCO_3	0.02046	-1.719%	8.81	-3.964	1729	0.7784
Cr-2	Na-HCO_3	0.00868	-0.07031%	6.58	-4.405	685.4	0.7358
Cr-3	Ca-HCO_3	0.009954	2.152%	6.96	-4.178	552.9	0.7966
Cr-4	Na-HCO_3	0.01604	-1.942%	28.84	-3.687	902	0.7914
Cr-5	Ca-HCO_3	0.006922	0.3588%	11.27	-4.255	377.8	0.8002
Cr-6	Na-Cl	0.01607	2.124%	32.48	-4.111	885.3	0.7905

Cr-7	Na-HCO_3	0.01289	2.332%	27.60	-3.83	763.9	0.7952
Ch-1	Ca-HCO_3	0.01523	4.132%	28.74	-3.803	819.2	0.8051
Ch-2	Ca-SO_4	0.01656	1.98%	29.33	-3.753	868.6	0.8064
Ch-3	Ca-HCO_3	0.005225	-0.7016%	3.02	-4.658	313.3	0.7877
Ch-4	Ca-HCO_3	0.005916	-3.51%	1.69	-3.931	393.6	0.8085
Ch-5	Ca-HCO_3	0.006159	-1.507%	1.65	-3.924	277.9	0.8029
Ch-6	Ca-HCO_3	0.004944	-1.151%	14.46	-3.751	392.3	0.7477
Ch-7	Ca-HCO_3	0.005553	-3.939%	1.24	-3.677	379.8	0.8176
Ch-8	Ca-HCO_3	0.006325	-2.756%	1.95	-3.724	415.9	0.8116
Ch-9	Ca-HCO_3	0.006168	-2.694%	2.97	-3.804	395.7	0.8063
Ch-10	Ca-HCO_3	0.005537	-1.1%	1.31	-3.658	343	0.8061
Ch-11	Ca-HCO_3	0.004781	-2.953%	14.34	-3.864	274.1	0.7841
Ch-12	Ca-HCO_3	0.004677	-4.937%	2.33	-3.593	285.2	0.7875
Ch-13	Na-SO_4	0.01409	-3.215%	24.66	-4.326	757.6	0.837
Ch-14	Ca-HCO_3	0.01252	-3.787%	18.04	-4.298	691.7	0.7842
Ch-15a	Ca-HCO_3	0.002034	-4.62%	2.63	-3.677	126	0.83
Ch-15b	Na-HCO_3	0.009084	1.004%	14.45	-3.821	498.8	0.8101
Ch-15c	Ca-HCO_3	0.01325	3.588%	20.96	-3.839	728.7	0.8176
Ch-16	Ca-HCO_3	0.006464	-0.6315%	7.42	-4.277	389	0.7904
Ch-17	Ca-Cl	0.02634	1.654%	27.45	-4.242	1555	0.798
Ch-18	Na-HCO_3	0.01182	3.126%	10.92	-4.381	765.6	0.7534

Table A.7: Simple Statistics for trace metals, dissolved oxygen, alkalinity, pH, Eh, and NO3- as N.

Simple Statistics						
Variable	N	Mean	Std Dev	Sum	Minimum	Maximum
Li	43	0.05291	0.04453	2.27530	0	0.16180
B	43	0.06344	0.12256	2.72800	0	0.66580
Mn	43	0.19997	0.53146	8.59880	0.0002000	3.29870
Fe	43	0.56630	1.88445	24.35080	0.00150	11.17000
Cu	43	0.00439	0.00773	0.18890	0	0.04520
Zn	43	0.01791	0.06874	0.77000	0	0.44870
Hg	43	0.00142	0.00366	0.06110	0	0.01550
Pb	43	0.0007047	0.00223	0.03030	0	0.01170
U	43	0.00787	0.00811	0.33860	0.0002000	0.03650
Ni	43	0.00156	0.00126	0.06710	0.0003000	0.00600
Co	43	0.0003233	0.0005149	0.01390	0	0.00290
As	43	0.0006605	0.0006849	0.02840	0	0.00250
Se	43	0.00130	0.00198	0.05610	0	0.00930
Mo	43	0.0005721	0.0007166	0.02460	0	0.00290
Cd	43	0.0000744	0.0002048	0.00320	0	0.00130
pH	43	7.10884	0.33350	305.68000	6.27000	7.96000
DO	43	3.53256	2.16980	151.90000	0.70000	9.26000
Alk	43	4.81186	2.82288	206.91000	0.69000	18.72000
Eh	43	0.79209	0.02155	34.06000	0.74000	0.84000
NO3asN	43	2.65605	5.41534	114.21000	0	21.85000